University of South Bohemia in České Budějovice
Faculty of Science

Modeling, parameter estimation, optimization and control of transport and reaction processes in bioreactors

Ph.D. Thesis

Ing. Václav Štumbauer

Study programme: Biophysics

Supervisor: Ing. Štěpán Papáček Ph.D.
Institute of Complex Systems, Faculty of Fisheries and Protection of Waters, University of South Bohemia

Supervisor/specialist: Ing. Karel Petera Ph.D.
Faculty of Mechanical Engineering, Czech Technical University in Prague

České Budějovice September 2016

This thesis should be cited as:

Štumbauer V., 2016: Modeling, parameter estimation, optimisation and control of transport and reaction processes in bioreactors. Ph.D. Thesis Series, No. 12. University of South Bohemia, Faculty of Science, České Budějovice, Czech Republic.

Annotation

With the significant potential of microalgae as a major biofuel source of the future, a considerable scientific attention is attracted towards the field of biotechnology and bioprocess engineering. Nevertheless the current photobioreactor (PBR) design methods are still too empirical. With this work I would like to promote the idea of designing a production system, such as a PBR, completely *in silico*, thus allowing for the *in silico* optimization and optimal control determination.

The thesis deals with the PBR modeling and simulation. It addresses two crucial issues in the current state-of-the-art PBR modeling. The first issue relevant to the deficiency of the currently available models - the incorrect or insufficient treatment of either the transport process modeling, the reaction modeling or the coupling between these two models. A correct treatment of both the transport and the reaction phenomena is proposed in the thesis - in the form of a unified modeling framework consisting of three interconnected parts - (i) the state system, (ii) the fluid-dynamic model and (iii) optimal control determination. The proposed model structure allows prediction of the PBR performance with respect to the modelled PBR size, geometry, operating conditions or a particular microalgae strain. The proposed unified modeling approach is applied to the case of the Couette-Taylor photobioreactor (CTBR) where it is used for the optimal control solution.

The PBR represents a complex multiscale problem and especially in the case of the production scale systems, the associated computational costs are paramount. This is the second crucial issue addressed in the thesis. With respect to the computational complexity, the fluid dynamics simulation is the most costly part of the PBR simulation. To model the fluid flow with the classical CFD (Computational Fluid Dynamics) methods inside a production scale PBR leads to an enormous grid size. This usually requires a parallel implementation of the solver but in the parallelization of the classical methods lies another relevant issue - that of the amount of data the individual nodes must interchange

with each other. The thesis addresses the performance relevant issues by proposing and evaluation alternative approaches to the fluid flow simulation. These approaches are more suitable to the parallel implementation than the classical methods because of their rather local character in comparison to the classical methods - namely the Lattice Boltzmann Method (LBM) for fluid flow, which is the primary focus of the thesis in this regard and alternatively also the discrete random walk based method (DRW).

As the outcome of the thesis I have developed and validated a new Lagrangian general modeling approach to the transport and reaction processes in PBR - a framework based on the Lattice Boltzmann method (LBM) and the model of the Photosynthetic Factory (PSF) that models correctly the transport and reaction processes and their coupling. Further I have implemented a software prototype based on the proposed modeling approach and validated this prototype on the case of the Coutte-Taylor PBR. I have also demonstrated that the modeling approach has a significant potential from the computational costs point of view by implementing and validating the software prototype on the parallel architecture of CUDA (Compute Unified Device Architecture). The current parallel implementation is approximately 20 times faster than the unparallized one and decreases thus significantly the iteration cycle of the PBR design process.

Declaration [in Czech]

Prohlašuji, že svoji disertační práci jsem vypracoval samostatně pouze s použitím pramenů a literatury uvedených v seznamu citované literatury. Prohlašuji, že v souladu s §47b zákona č. 111/1998 Sb. v platném znění souhlasím se zveřejněním své disertační práce, a to v úpravě vzniklé vypuštěním vyznačených částí archivovaných Přírodovědeckou fakultou elektronickou cestou ve veřejně přstupné části databáze STAG provozované Jihočeskou univerzitou v Českých Budějovicích na jejích internetových stránkách, a to se zachováním mého autorského práva k odevzdanému textu této kvalifikační práce. Souhlasím dále s tím, aby toutéž elektronickou cestou byly v souladu s uvedeným ustanovením zákona č. 111/1998 Sb. zveřejněny posudky školitele a oponentů práce i záznam o průběhu a výsledku obhajoby kvalifikační práce. Rovněž souhlasím s porovnáním textu mé kvalifikační práce s databází kvalifikačních prací Theses.cz provozovanou Národním registrem vysokoškolských kvalifikačních prací a systémem na odhalování plagiátů.

Acknowledgments

Here I would like to express my gratitude to all the people involved in the PhD program at the former Institute of Physical Biology for the beautiful experience they were all part of.

Special thanks belongs primarily to my supervisor Dr. Štěpán Papáček who was not only willing to take me on this journey - despite the fact that I had a family and a full-time job in a completely different field already - but also patient enough to persevere with me till the end.

Another person from the field not to be forgotten is Dr. Karel Petera from the Department of Process Engineering, Faculty of Mechanical Engineering, Czech Technical University in Prague, who shared with me a lot of valuable insights on the topic.

I am also grateful to my wife Tereza, who supported me relentlessly despite being busy with two children and having a demanding job of her own.

Thank You

Václav Štumbauer

List of the papers

This thesis is based on the following papers, first three of which have been already published and where the thesis's author is either the main author or a coauthor. The papers are listed chronologically.

- **Papáček Š., Štumbauer V., Štys D., Petera K., Matonoha C.: Growth impact of hydrodynamic dispersion in a Couette-Taylor bioreactor.**
  Mathematical and Computer Modelling, 7-8 (54) (2011), 1791–1795, (IF=2.22)

  Václav Štumbauer helped with the hydrodynamic dispersion based simulations, with the Couette-Taylor dispersion coefficient function determination and validation and participated in the writing of the manuscript.

- **Papáček Š., Matonoha C., Štumbauer V., Štys D.: Modelling and simulation of photosynthetic microorganism growth: random walk vs. finite difference method.**
  Mathematics and Computers in Simulation, 10 (82) (2012), 2022–2032, (IF=1.22)

  Václav Štumbauer implemented the random walk based bioreactor simulation software and supplied the random walk based simulation results. He also participated in the writing of the manuscript.

- **Štumbauer V., Petera K., Štys D.: Lattice Boltzmann method in bioreactor design and simulation**
  Mathematical and Computer Modelling, 7-8 (57) (2013), 1913–1918, (IF=2.84)
  Václav Štumbauer wrote the manuscript, implemented all the relevant simulation software on all the target platforms and supplied all the relevant simulation data.

- **Papáček Š, Jablonský J., Štumbauer V., Petera K., Rehák B., Matonoha C.: Modeling and optimization of microalgae growth in photobioreactors: a multidisciplinary multiscale problem**
  submitted manuscript
  Václav Štumbauer participated in writing the manuscript, which is a generalized summarization/review of the bioreactor model-based design process and builds upon the previous work.

Contents

Chapter 1

Introduction

Microalgae attract a lot of scientific interest because of its promising potential in wide range of applications, which is the reason of the extensive research activity in the field of photobioreactors (PBR) - devices for the artificial photoautotrophic cultivation of the microalgae, whose modeling is the primary purpose of this work.

Microalgae are mostly unicellular eukaryotic or prokaryotic photosynthetic microorganisms living in both marine and fresh-water environments and even in the soil. It may also exist as a group of cells, but it does not exist as a multicellular organism as such.

Microalgae are a diverse and large family [1] of photosynthetic microorganisms and thus offer a wide spectrum of, still mostly uncharted, bioactive compounds [2]. Due to its diversity, it is believed to contain many possible novel pharmaceuticals and other bioactive compounds and microalgae are thus subject to various screening programs - see e.g. [3].

It is also due to the high energy content, that microalgae are considered a promising source of biofuels [4, 5], which naturally attracts a lot of scientific attention due to the ever-increasing demand for the fuels and the associated commercial potential. There are several advantages that microalgae have over the terrestrial plants as a source of renewable energy. First, it does not compete with agricultural crops and thus it does not place any further pressure on the prices of the basic agricultural commodities. Second, the photosynthetic efficiency of the fast growing microalgae greatly exceeds the photosynthetic efficiency of the terrestrial plants. Also, microalgae are rich in lipids and starch. On the other hand, with respect to the biofuels, it should be also noted, that be-

cause of the limitation on the culture density due to the light requirements and high water content/energetically demanding drying process, the costs associated with microalgae cultivation and harvesting in comparison to the terrestrial plants are still substantial and need to be addressed yet. While the currently sensitive topic of biofuels may receive the most attention, of a significant interest are also the environmental applications, where microalgae may be used for bio remediation [6] - e.g. heavy metals removal, waste water treatment and CO2 sequestration. Further applications may be found in aquaculture [7] and cosmetic industry [8].

In its natural habitat, microalgae do not occur in such a culture density, that would allow for economically feasible harvesting. Artificial microalgae cultivation systems are thus also subject of the scientific research. As of now, the microalgae are cultivated either in large open outdoor systems, where there are currently several predominant types [9] - large open ponds, circular ponds with a mixing arm and raceways. Or in a closed cultivation system - in a bioreactor [10, 11], or more specifically, a photobioreactor (PBR) in the case of the closed-system phototrophic cultivation. PBR and its *in silico* design is also the research subject of this thesis.

Despite the scientific interest, the process of bioreactor design is still rather empirical and a complete computer based modeling approach or software is still unavailable [10]. Such an approach would allow for cheaper design process and better parameters and operating conditions optimization. The unavailability of such a *in silico* PBR design tool has several reasons. The field of biotechnology is currently used to the empirical or semi-empirical approaches to the photo/bioreactor design and there exists a substantial group of biotechnological scientists believing in the superiority of such a design method. Apart from this, rather philosophical issue, the computer based PBR design is complicated due to the complexity of the relevant processes and their interplay and last but not least also due to the immense computational complexity involved in the simulation of a production-scale PBR. The performance related design issues are another important point this works concentrates on.

The ultimate aim this work contributes to, i.e. being able to predict **in reasonable time** the microalgae growth rate for a particular PBR in question - respecting the geometry and scale of the device as well as mixing mechanism and its intensity, illumination setup etc., is of yet more importance when it comes to the PBR optimization, where the search for the optimal device parameters and optimal operating conditions may involve many simulation runs in order to explore the relevant parameter space.

1.1 Microalgae cultivation

1.1.1 Principles

Light

The primary influencing factor in the phototrophic microalgae cultivation is definitely light [10]. Economical feasibility of any cultivation system commands an artificially high culture concentration and, apart from some special cases, a large cultivation volume. Since the light penetrating into the culture is attenuated exponentially in dependence on the penetrated depth, the efficient light distribution among the cultivated cells introduces a necessity of mixing the culture, so that all the cells are exposed to the light relatively evenly and none of them are either light-limited or light-inhibited. The exponential attenuation may be expressed by the Beer-Lambert law as follows:

$$I_d = I_0 exp(-Ad) \tag{1.1}$$

where I_0 stands for the culture surface irradiance intensity, I_d for the light intensity at the depth d and A stands for the absorbance - i.e. optical density of the culture.

It is worth noting, that there exist more complex approaches to the light distribution modeling in bioreactors than those, that are based on the Beer-Lambert law, since this law may be considered inaccurate with respect to its aggregated treatment of the two underlying optical phenomena - the absorption and the scattering. For the details on these alternative modeling approaches please see e.g. [12, 13, 14].

The currently most accurate models are the diffuse light distribution models which account for the effects of absorption of the light by the pigments, scattering of the light by cells and other present particles and also incorporate the geometry of the light source and PBR [15, 16]. In [16] it has been shown that these models can be employed in the productivity prediction of the outdoor column photobioreactor with varying external conditions. A disadvantage of this light distribution modeling approach is the requirement of a huge amount of experimental data.

Relying solely on the Beer-Lambert law, as was done in the published papers, the light distribution model for the cylindrical Couette-Taylor photobioreactor (CTBR) with radial illumination - a model corresponding to our laboratory setup and thus a model which has been used extensively in the published papers - may be formalized as follows:

$$I_r = \frac{I_0 R}{r}[exp(-A(R-r)) + exp(-A(R+r))] \tag{1.2}$$

where r stands for the distance from the outer surface in the radial axis and R stands for the outer radius.

Flashing light effect

Important, from the PBR design point of view, is also the capacity of the microalgae to grow under sufficiently fast light intensity fluctuations as if it was illuminated by a light source of constant intensity. This flashing-light effect was described in [17] and further model based clarification has been presented in [18]. This effect is crucial for the possibility of cultivation of dense cultures in PBRs, which are, as further explained, being mixed and where cultivated microalgae travels between the dark and the photic region of the PBR. The efficiency of the photosynthesis grows hyperbolically with the increasing frequency of the light/dark cycles, reaching its maximum value when the light/dark cycles frequency matches that of the photosystem II electron's turnover rate [19].

Naturally, not only the frequency, but also the duty cycle and light intensity in the photic phase play an important role with respect to the photosynthetic activity [20, 21].

Mixing

It is not only the distribution of light that makes the suspension mixing in the PBR necessary. The phototrophically cultivated microalgae do also require a sufficient concentration of the nutrients, sufficient supply of the carbon dioxide and removal of the products, such as e.g. oxygen. Without mixing, concentration gradients would occur and thus the mixing plays an essential role in the processes of mass-transfer and gas-exchange [10, 22].

There are various approaches to mixing the suspension with microalgae [11] - from the simplest mechanical approach to the more indirect approaches as e.g. in the case of the airlift or bubble column photobioreactors. Another alternative approach to mixing is a rotating wall in the case of the cylindrical device - the so-called Couette-Taylor photobioreactor (CTBR), first proposed in the [23], whose advantage are the well defined flow regimes and shear stress at the lower Reynolds numbers - i.e. before the turbulent regime is reached.

Mixing has not only the positive effects on the cell culture growth. With increasing intensity it may become detrimental to the cultivated cells in the form of the shear stress that the cells are exposed to. The microalgae are very diverse

and there are significant differences between different strains with respect to the levels of the shear forces they can tolerate without detrimental effects on the cell physiology or the growth.

There is currently a general unavailability of the microalgae growth models that would incorporate the shear stress. Nevertheless, there exist studies analyzing the dependence of the microalgae growth on the shear forces the microalgae are exposed to. In [24] the authors identify as critical, in the case of the *Phaeodactylum tricornutum*, values of shear rates γ exceeding the value of 7000 s^{-1} and the turbulent micro eddies of smaller sizes than 45 μm, relating the micro eddies size to the turbulence dissipation rate as follows:

$$l = (\frac{\nu}{\rho})^{\frac{3}{4}} \epsilon^{-\frac{1}{4}} \tag{1.3}$$

where ν stands for the suspension viscosity, ρ for the fluid density and ϵ for the turbulence dissipation rate. In [25] the impact of the shear stress on the cell viability was studied in a combination of a rheometer and a special shearing device in the case of the *Chaetoceros muelleri*. It is noteworthy that such a device is in principal very similar to the Couette-Taylor photobioreactor (see further), that is a research subject in our laboratory. It is the very well definable and controllable shear stress inside the device, if the laminar flow regime is sustained, that makes this device very interesting with respect to the fragile strains cultivation and shear stress growth rate dependence assessment. With respect to the shear stress, it must be noted that the artificial cultures must be aerated with $CO2$ which is another source of the shear stress the cultivated microalgae are exposed to - through their contact with the bubbles [26, 27].

The aforementioned leads to the necessity of adjusting either the whole PBR design or the operating conditions according to the microalgal strain that is to be cultivated.

1.1.2 Cultivation systems

The systems for microalgae cultivation vary widely in many respects. The topmost categorization is based on the fact, whether the particular system in question is either an open system - where the mass-transfer between the system and surrounding is possible, or a closed system where such a transfer is not possible [10]. While the open cultivation systems offer the advantage of lower construction and operating costs in comparison to the closed systems, they are not suited well to the cultivation of all the microalgal strains, but rather those that either grow under extreme conditions or grow extremely fast and are thus

resistant to the culture contamination. Examples of the strains, that may be cultivated in the open systems are e.g. *Dunaliella* [28] which grows under highly saline conditions or *Chlorella* [29] which grows rapidly.

Another distinction can be made from the cultivation regime, the system in question provides. The microalgae may be cultivated either in a batch or semi-batch regime, where the necessary nutrients, inoculum etc. are put into the system at discrete time intervals. The product is removed at the discrete time intervals as well. Examples of such a cultivation regime are e.g. the air-lift [30], bubble column [30] and Couette-Taylor photobioreactors [23]. As opposed to the batch or semi-batch cultivation regime, in a continuous cultivation regime, the relevant concentrations are adjusted adaptively and the product is thus removed continuously.

In either case a cultivation system must provide the cultivated culture with optimal growth conditions and this can be achieved more easily in the case of a closed system, because of the better control of the cultivation conditions.

Closed systems

In the case of the closed cultivation systems we deal either with the photobioreactors (PBRs) in the case of the autotrophic and mixotrophic modes of cultivation or with the fermenters in the case of the heterotrophic mode of cultivation, where the light is not required. This thesis concentrates on the photoautotrophic microalgae cultivation, ant the subsequent text deals with the PBRs only.

Unlike in the case of an open system, a PBR as a closed system offers much better control over the environment and operating conditions, which makes it possible to cultivate the microalgae under well-defined/optimal and relatively stable conditions.

The closed systems are economically much more demanding [31] than the open systems such as open ponds or raceways, but an open system is not an universal solution for all the microalgal species. Generally a closed system is to be used, where the mono-culture growth under well defined cultivation conditions is required.

The most popular enclosed PBR design solutions are the flat panel PBRs and tubular PBRs [32]. In [33] the modeling of the flat panel reactor based on the random walk method and finite differences method is presented. In [34] the special case of the tubular photobioreactor accompanied by the Fresnel lenses - leading to the artificially high culture irradiance - is presented.

A particular example of a closed cultivation device is the **Couette-Taylor photobioreactor (CTBR)**, which has been used as the main validation case

for the bioreactor modeling software developed in the scope of this thesis - [35, 36].

The device, first proposed for microalgal cultivation in [23], is comprised of two concentric cylinders, where the rotation of the inner cylinder provides the necessary mixing to ensure the mass-transfer, gas-exchange and intermittent illumination of the cultivated culture. The device has been chosen as the main validation use case because it is a research subject of our laboratory and because it exhibits interesting properties with respect to well defined hydrodynamic stress the cultivated culture is exposed to and offers the possibility of shear stress control by varying the rotation frequency of the rotating cylinder. The device has been also physically constructed and was subject to experimental work with respect to the microalgal culture growth measurement under various physiological circumstances - mainly under varying shear stress conditions.

A particular configuration of the device, corresponding to the experimental device used in our research facility, is schematically depicted in figure 1.1. The system of two concentric vertical cylinders has the inner cylinder connected through a drive shaft with a motor with adjustable rotation rate (a). A system of light belts (d) is coiled around the outer cylinder (b), providing thus a symmetrical and controllable homogeneous light source. The suspension with culture (b) is put into the device at the cultivation start and collected at the end - the device is operated in the batch regime. Carbon is provided by bubbling the suspension with a 5% mixture CO_2 and air.

Based on the angular velocity of the inner cylinder and on the inner and outer cylinder diameter, different fluid flow patterns occur in the cylindrical gap. First a simple laminar Couette flow occurs. With increasing angular velocity of the inner cylinder a Taylor vortex flow is reached [37], which is subsequently transformed into the wavy vortex flow. Further increasing the cylinder angular velocity leads to the onset of the turbulence. In [38], it has been demonstrated that even in the turbulent flow regimes, there is an increase in the light/dark cycle frequency for the cultivated microalgal cells relevant to the increase in the angular velocity of the mixing cylinder.

The transitions between the different characteristic fluid flow patterns are best described by the so-called Taylor number, which may be defined as follows:

$$Ta = \frac{\Omega^2 R_1 (R_2 - R_1)^3}{\nu^2} \tag{1.4}$$

where Ω stands for the characteristic angular velocity, R_2 for the internal radius of the outer cylinder and R_1 for the external radius of the inner cylinder. The critical Taylor number $Ta_c = 41.3$ marks the transition of the laminar

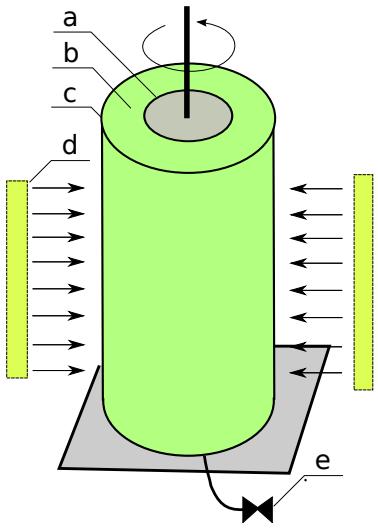

Figure 1.1: Couette-Taylor photobioreactor depicted schematically. *a - inner cylinder connected through a drive shaft with a motor governed by speed regulator, b - suspension is placed inside the cylindrical gap. While it is not shown in the depicted image, the gap is capped and only degassing is allowed through a valve leading through the cap, c - outer cylinder must let the maximum photosynthetically active light through, so that it can reach the cultivated culture, d - artificial illumination is required for the higher/artificial culture densities, e - the system is bubbled with* 5% *mixture of* CO_2 *with air*

flow to the vortex flow. Further increase in the Taylor number leads to the vawy vortex flow under the assumption that the following condition is fulfilled: $\frac{R_2}{R_1} < 1.4$ [39].

1.2 PBR Design

This work concentrates primarily on the photobioreactors, a closed systems where the microalgae are cultivated in the photoautotrophic mode and where light plays the most important role in the cultivation process. Under the assumption that no other relevant parameters are limiting, light is the single governing parameter for microalgae growth [10].

Although different microalgal strains may grow under wide range of environmental conditions, productivity of a cultivation process may be severely impacted when the environmental conditions such as temperature or pH are not in the vicinity of its optimal value for the given strain - see e.g. [40]. With closed systems, as is the case of PBR, there is much better control over the operating conditions such as temperature and pH. The primary concern in the case of a closed system is thus the light distribution and the relevant suspension mixing [10, 22]. Mixing mechanism and its intensity should allow for the optimal mass-transfer and gas-exchange and formostly for the optimal light distribution to the cultivated microalgal cells, while at the same time it should not be detrimental to the cultivated cells by exposing them to excessive levels of shear stress.

Enormous diversity of the microalgae also complicates the matter of PBR design. The attributes of a particular specie in question are of paramount importance when it comes to the optimal mixing mechanism and intensity and the relevant optimal irradiance. Various species may also yield various products under different forms of limitation. And thus the PBR design aim may be the maximization not of the overall product, but e.g. a production of a particular metabolite, which may subsequently require yet different operating conditions - e.g. exposing the microalgae to a certain minimal level of the shear stress or light stress [41].

1.3 PBR modeling

PBR design process has a clear objective - to determine the optimal device parameters and operating conditions allowing for productivity maximization for a particular strain or a particular product/metabolite in question. This leads

to the necessity of being able to simulate the productivity of a system with a given set of parameters - so that the optimal system parameters and operating conditions may be found. In other words a reliable PBR model or modeling framework is required in the PBR design.

PBR modeling is, from the computational point of view, an enormously complicated task. Generally, it deals with the modeling of a three dimensional multiphase and multiscale problem and it is further complicated by the spatial scale of the simulated domain when modeling a production scale PBR.

PBR model must deal with the fast transport processes coupled to the slower processes of the reaction model - the biological processes, which, in the case of the phototrophic organisms, also operate on multiple time scales [43, 44, 45]. In general, both models - of the transport and of the reaction - cannot be separated in a trivial manner. The transport model yields not only the information about the trajectories of the cultivated microalgae - thus allowing for the computation of the cells' irradiance at any given moment, but it also gives crucial information regarding the mass-transfer, gas-exchange and shear stresses to which are the cultivated cells subjected at a particular moment.

1.3.1 Transport modeling

In general the transport processes inside the PBR are governed by the incompressible Navier-Stokes equations. Navier-Stokes(NS) equations are partial nonlinear differential equations of the second order constraining the pressure scalar and velocity vector at a given point in the fluid. Their solution leads to obtaining the velocity field and pressure throughout the fluid. While NS equations may be formulated with regard to the compressibility of a fluid, it is unnecessary for the presented aims and only the incompressible NS equations have relevance to the following text.

The incompressible form of the Navier-Stokes equations along with the relevant continuity equation may be written as follows:

$$\rho\left(\frac{\partial \mathbf{v}}{\partial t} + \mathbf{v}\cdot\nabla\mathbf{v}\right) = -\nabla p + \mu\nabla^2\mathbf{v} + \mathbf{f} \tag{1.5}$$

$$\frac{\partial \rho}{\partial t} + \nabla\cdot(\rho\mathbf{v}) = \nabla\cdot\mathbf{v} = 0 \tag{1.6}$$

Navier-Stokes based computerized solution of the transport leads to the discretization of the PBR volume with one one the available methods (e.g. a Finite Volume Method or Finite Difference Method) and solving the discretized NS system.

NS equations in their basic form are not suited well for the description of the turbulent flow regime because of the very small spatial and temporal scales that need to be reflected in the discretization mesh - the so-called direct numerical simulation (DNS) that uses the NS equations directly without a turbulent model must reflect all the spatial scales from the smallest Kolmogorov microscales up to the global scale. The mesh size in DNS is constrained by the Reynolds number Re as follows:

$$N^3 >= Re^{\frac{9}{4}} \tag{1.7}$$

where N^3 corresponds to the number of mesh points. It is thus computationally unfeasible to perform DNS for the higher Raynold numbers, especially in the case of a non-stationary flow.

Different approaches thus exist to approach the turbulence in the scope of the NS equations - Reynolds-averaged Navier-Stokes(RANS) equations or Large Eddy Simulation(LES) being the most notable adjustments to the NS equations with respect to turbulent flow modeling. While RANS is based on time-averaging, the LES approach is based on the idea of a low-pass filter used to remove the spatial scales that are under the resolution capability of a given discrete mesh.

One of the most common methods to approach the turbulence in regard to the NS equations is the k-ϵ turbulence model family. The k-ϵ models (as well as e.g. the k-ω) introduce two more transport partial differential equations with transported variables being the turbulent kinetic energy k and the turbulent dissipation ϵ.

With relevance to the field of biotechnology, in [46] a RNG (Renormalization - group) k-ϵ model has been successfully employed to obtain the trajectories of the cultivated microalgal cells inside the Couette-Taylor photobioreactor.

With respect to the performance potential of the NS based methods on the parallel computational architectures, a certain non-negligible amount of data must be interchanged between the individual nodes. This is the reason, why in this work, two alternative approaches to the transport solution, in my opinion better suited for parallel implementation, have been studied - the Lattice Boltzmann Method (LBM) [36] for fluid flow and a random walk (RW) based method [33].

The Lattice Boltzmann Method

The Lattice Boltzmann Method (LBM) for fluid flow simulation [47, 48] attracts a lot of attention due to its capability to simulate the complex flows, its perfor-

mance potential and straight-forward implementation. The method is based on the streaming and collision of the particles, or particle densities, on a discrete mesh. It is also noteworthy that the NS equations can be recovered from the LBM [47]. Basically the LBM method may be viewed as a simplified form of the Boltzmann's transport equation with reduction in the number of particles, in space - the particles are confined to a discrete lattice and in time - the particle positions are recalculated at discrete time steps. The possible momenta are also constrained to a set of discrete directions and relevant magnitudes.

At first, the LBM method was developed for regular lattices, where different discretizing schemes have been developed, differing in the number of supported directions and dimensions. In [49] a classification of these schemes was introduced. In the case of the two dimensional simulation, the D2Q9 scheme, constraining the momenta to 9 discrete directions and magnitudes, is probably the most employed. The same applies to the D3Q19 scheme, which constrains the momenta to 19 discrete directions and magnitudes in the three dimensional simulations and is commonly employed as a trade-off between the computational costs and accuracy. The D3Q19 lattice structure is depicted in figure 1.2. In this scheme, there are 19 directional vectors $\mathbf{e_1}$ - $\mathbf{e_{19}}$. Vectors 1-18 connect the node to adjacent nodes, vector $\mathbf{e_{19}}$ corresponds to the particles at rest.

LBM operates in discrete time steps. Every step, the particles are streamed to the adjacent nodes of the lattice - the so-called streaming step and then the node-local collision is evaluated, leading to the adjustment of the particle densities for each of the discrete directions.

This can be expressed for the so-called single-relaxation-time (SRT) model in the following form [48]:

$$f_a(\mathbf{x} + \mathbf{e}_a \Delta t, t + \Delta t) = f_a(\mathbf{x}, t) - \frac{[f_a(\mathbf{x}, t) - f_a^{eq}(\mathbf{x}, t)]}{\tau} \tag{1.8}$$

where a denotes the relevant discrete direction, f_a corresponds to the density distribution function in the direction a, $\mathbf{e}_a$ is a particle velocity vector in the direction a, Δt is a time step and τ is the 'single-relaxation-time'(SRT) - timely constant expressing the relaxation rate to the local equilibrium. This constant is related to the kinematic viscosity as follows: $\nu = \frac{1}{3}(\tau - \frac{1}{2})$.

Particle equilibrium density in the direction a at the lattice site $\mathbf{x}$ is denoted as $f_a^{eq}(\mathbf{x}, t)$ and in the BGK SRT model is calculated as follows:

$$f_a^{eq}(\mathbf{x}, t) = w_a \rho(\mathbf{x}, t) \left[1 + \frac{\mathbf{e}_a \cdot \mathbf{u}(\mathbf{x}, \mathbf{t})}{c_s^2} + \frac{(\mathbf{e}_a \cdot \mathbf{u}(\mathbf{x}, t))^2}{2c_s^4} - \frac{\mathbf{u}^2(\mathbf{x}, t)}{2c_s^2} \right] \tag{1.9}$$

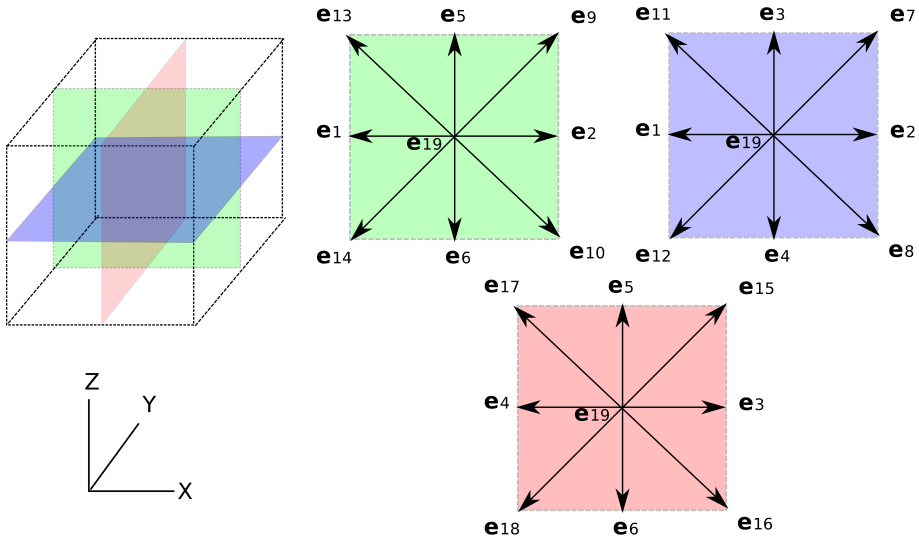

Figure 1.2: LBM D3Q19 lattice structure

where $\mathbf{u}(\mathbf{x}, t)$ stands for macroscopic velocity, ρ for the macroscopic density, c_s for lattice speed of sound $c_s = \frac{1}{\sqrt{3}}$ and w_a for weighting coefficients, which specifically for the case of the D3Q19 model have the following values:

$$w_a = \begin{cases} \frac{2}{36} & 1 \leq a \leq 6 \\ \frac{1}{36} & 7 \leq a \leq 18 \\ \frac{12}{36} & a = 19 \end{cases} \tag{1.10}$$

Macroscopic velocity vector and macroscopic density are related to the density distribution function as follows:

$$\rho(\mathbf{x}, t) = \sum_a f_a \tag{1.11}$$

$$\mathbf{u}(\mathbf{x}, t) = \frac{1}{\rho(\mathbf{x}, t)} \sum_a f_a \mathbf{e_a} \tag{1.12}$$

Boundary conditions treatment

One of the advantages of the Lattice-Boltzmann method is its capability to simulate very complex flow domains [48] and a significant effort has been

already invested in the boundary conditions analysis. The most simple and widely adopted is the so-called bounce back boundary condition (BBC) [47], which is based on the idea of particle flow densities being consumed by the solid wall and then reemerging with the inverted velocity vector. The weaknesses of the BBC have been demonstrated in [50, 51] and in [52] it has been shown that with a proper position of the bounce-back lattice nodes and selection of τ close to 1 [52] leads to satisfactory results. With BBC a second order accuracy may be obtained if the bounce-back nodes are fictively placed in the middle between the last fluid and first solid node - the so-called half-way bounce-back boundary condition.

In [53] a straight wall velocity and pressure boundaries treatment based on the bounce-back of the non-equilibrium parts of the distribution function has been proposed.

The aforementioned boundary treatments can cover a wide range of scenarios but unfortunately are insufficient for the simulation of the rotating inner wall - i.e. curved velocity boundary - in the case of CTBR. As it has already been elaborated in our paper [36], a special treatment of the curved velocity boundary is required in order to preserve the accuracy and stability of the solution.

Multiphase and multicomponent flows

In real PBR we deal with a multiphase and multicomponent flow. In order to simulate such a flow, introduction of the external forces into LBM is necessary. Impact of the external force $\mathbf{F}$ is introduced through the adjustment to the macroscopic velocity vector that is used in the calculation of the equilibrium particle density function $\mathbf{f^{eq}}$ as follows [48]:

$$\mathbf{u_{eq}} = \mathbf{u} + \frac{\tau \mathbf{F}}{\rho} \tag{1.13}$$

$$f_a^{eq}(\mathbf{x}, t) = w_a \rho(\mathbf{x}, t) \left[1 + \frac{\mathbf{e}_a \cdot \mathbf{u_{eq}}(\mathbf{x}, \mathbf{t})}{c_s^2} + \frac{(\mathbf{e}_a \cdot \mathbf{u_{eq}}(\mathbf{x}, t))^2}{2c_s^4} - \frac{\mathbf{u_{eq}}^2(\mathbf{x}, t)}{2c_s^2} \right] \tag{1.14}$$

Interactions between the particles are necessary in order to incorporate multiple phases and components into the LBM. Based on the interaction with the adjacent nodes, the inter-particle interaction may be formulated as follows ([48]):

$$\mathbf{F}(\mathbf{x}, t) = -G\psi(\mathbf{x}, t) \sum_a w_a \psi(\mathbf{x} + \mathbf{e_a}\Delta t, t)\mathbf{e_a} \tag{1.15}$$

here G represents the interaction strength and ψ the interaction potential. In [54] the following form of the interaction potential is proposed for the multiphase single component fluid flows:

$$\psi(\rho) = \psi_0 exp(\frac{-\rho_0}{\rho}) \tag{1.16}$$

Various other forms of the inter-particle potential are in common use - see e.g. [55, 56].

In order to incorporate other components into the fluid flow simulation, the LBM approach is replicated to the individual components and componental interaction is modeled again by the inter-particle interactions [48]. If the individual components are denoted by σ, the macroscopic velocities of the individual components $\mathbf{u}_\sigma$, coupled macroscopic velocity $\mathbf{u}'$, component-specific macroscopic densities ρ_σ, component-specific relaxation parameter τ_σ and component-specific microscopic particle densities f_a^σ, then for the case of the multicomponent flow the following relations are valid:

$$\mathbf{u}_\sigma = \frac{1}{\rho_\sigma} \sum_a f_a^\sigma \mathbf{e}_a \tag{1.17}$$

$$\mathbf{u}' = \frac{\sum_\sigma \frac{1}{\tau_\sigma} \sum_a f_a^\sigma \mathbf{e}_a}{\sum_\sigma \frac{1}{\tau_\sigma} \rho_\sigma} \tag{1.18}$$

$$\rho_\sigma = \sum_a f_a^\sigma \tag{1.19}$$

and for the force exerted on the individual fluid component $\mathbf{F}_\sigma$ holds the following relation [48]:

$$\mathbf{F}_\sigma(\mathbf{x}, t) = -G\psi_\sigma(\mathbf{x}, t) \sum_a w_a \psi_{\bar{\sigma}}(\mathbf{x} + \mathbf{e_a}\Delta t, t)\mathbf{e_a} \tag{1.20}$$

where $\overline{\sigma}$ denotes the other fluid component. The macroscopic velocity used for the collision evaluation of the component σ, denoted as $\mathbf{u}_\sigma^{eq}$, is then evaluated as follows

$$\mathbf{u}_\sigma^{eq} = \mathbf{u}' + \frac{\tau_\sigma \mathbf{F}_\sigma}{\rho_\sigma} \tag{1.21}$$

LBM discretization

The LBM simulation operates on the discrete lattice and in discrete time steps. If we denote the discrete spatial unit as Δx and the discrete time step as Δt, the following relation is valid between the relaxation rate τ and viscosity ν ([57]):

$$\nu = \frac{\Delta x^2}{3\Delta t}(\tau - 0.5) \tag{1.22}$$

If we further denote the characteristic physical scale as L, the characteristic macroscopic velocity as U and the number of lattice nodes along the characteristic scale as $N = \frac{L}{\Delta x}$ we obtain the relation for the Mach number Ma:

$$Ma = \frac{\Delta x}{L\sqrt{3}}(\tau - 0.5)Re \tag{1.23}$$

LBM can simulate the incompressible fluid flow relatively accurately under the condition of keeping the Mach number low and the LBM error is in the order of Ma^2 [57]. This implies that the number of lattice nodes N along the characteristic scale and the relaxation rate τ must be chosen with respect to keeping the Mach number Ma low.

Further in order to obtain correspondence between the real physical system and the discrete LBM simulation, the Reynolds number defined by the physical characteristic scale L and velocity U must be equal to the 'lattice' Reynolds number based on the number of lattice nodes N:

$$Re = \frac{UL}{\nu} = \frac{uN}{\nu} \tag{1.24}$$

The lattice velocity u should be at the order of approx. $u <= 0.1$ and the other parameters are then be chosen arbitrarily - based on the preceding relations, so that the stability and accuracy are ensured and the simulated system corresponds to the physical system.

Discrete Phase Modeling

The discrete phase modeling, in the context of PBRs, yields the microalgal cells' (further denoted as particles in the scope of this section) positions and trajectories which are necessary primarily for the evaluation of the light intensity the individual cells encounter in PBR - light being the primary input for the growth/reaction model. Although also Eulerian based approaches to the particle tracking exist, especially with respect to the focus on the Lattice Boltzmann

fluid flow simulation method, only the Lagrangian based approaches tracking the positions of the individual cells are described further.

As shown e.g. in [58], even a very dense microalgal suspension has a very low volumetric ratio of the dispersed solid phase to the fluid phase. Furthermore in [59] an impact of the microalgal proliferation as well as of the exopolysascharide released by the cells [60] on the suspension viscosity is evaluated, reaching the conclusion that the change in the viscosity may be neglected unless a longer experiments ($>$ 10 days - [61]) with higher concentration of exopolysascharides were considered. This leads to the conclusion that a one-way coupling between the fluid phase and the dispersed solid phase is sufficient.

The easiest way of tracking the particles in the suspension would be a simple alignment of the particle trajectories with the local velocity field, but especially in the case of turbulent flows, such a model is not too realistic. Better results, when modeling a turbulent dispersion of particles, may be obtained by e.g. the particle cloud method or by the discrete random walk (DRW) based stochastic particle tracking - see e.g. [62].

In the case of the stochastic tracking, every injected particle is tracked multiple times in order to obtain a reasonable statistic sample. Every time step, particle velocity is adjusted as follows:

$$u_i = \bar{u_i} + N\sqrt{\frac{2k}{3}} \tag{1.25}$$

In this relation u_i stands for the particle velocity component in the direction of i, $\bar{u_i}$ stands for the flow field velocity, N for the normally distributed random variable and k represents the turbulent kinetic energy.

The particles dispersed in the fluid phase may encounter the physical boundaries of the simulated domain, they may come into contact with the dispersed gaseous phase ($CO2$ bubbles) or with each other. In [63], the importance of modeling the interaction between the dispersed gaseous and solid phases have been demonstrated.

1.3.2 Reaction modeling

In the case of the phototrophic organisms growth modeling - i.e. a reaction modeling of the PBR, the light becomes often the sole determinant factor, since all the other influencing parameters, such as nutrient concentrations, temperature etc., may be kept relatively easily at their optimal values. The goal of a reaction model is thus in the case of the PBR often reduced to the evaluation

the specific growth rate μ or productivity P of the cultivated culture based on the light intensity.

The cultures in the cultivation systems must be unnaturally dense in order for the biotechnological process to be economically feasible. The dense and thick culture also means that not all the cells are exposed to the sufficient light, i.e. that would support the photosynthetic growth and positive net productivity, all the time. The volume of the photobioreactor may be in the simplest of terms divided into two zones - the photic zone, where there is sufficient light available to support the photosynthesis/growth and the dark zone, where the light is insufficient. With the necessary mixing, the cells traverse between these two zones and thus encounter various light intensities over the course of the time. These dynamic effects simply cannot be captured by the static nature of the so-called P-I curve [64], which is still used extensively in the biotechnology. The P-I curve models the steady-state dependence of the productivity P on the average/constant light intensity I, that the culture es exposed to.

Much better suited to the dynamic nature of PBR cultivation is a Lagrangian time-resolved model, that is capable of taking into account the inherent dynamic nature of the underlying physiological processes (i.e. photosynthesis relevant processes of microalgae) and building on the coupling with the fluid dynamics. In these models the timely course of the light intensity and possibly also other phenomena as e.g. shear stress and temperature is captured and used as a model's input.

It is in this way, that the model of the so-called Photo Synthetic Factory (PSF), firstly introduced in [43, 44], is built. The model's sole input parameter is the light intensity as a function of time. It is the light intensity the individual cell or a given volume (based on the PSF interpretation as either a system of ordinary or stochastic differential equations) is exposed to. The model mimics the physiological processes of photo-limitation and photo-inhibition and covers also the dynamic effects of the flashing-light effect [65]. The Model of PSF, as used throughout the presented papers, is based on the further improvements and analysis of the original model as presented in [45, 66, 67, 68, 69].

To formalize the model of PSF, it is comprised of 3 ODEs and a normalizing condition:

$$1 = x_A + x_I + x_R \tag{1.26}$$

$$\frac{dx_R}{dt} = \gamma x_A + \delta x_I - \alpha u x_R \tag{1.27}$$

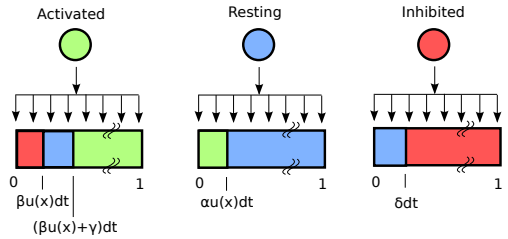

Figure 1.3: Stochastic treatment of PSF - photo state switching of microalgae cells

$$\frac{dx_A}{dt} = -\gamma x_A + \alpha u x_R - \beta u x_A \tag{1.28}$$

$$\frac{dx_I}{dt} = -\delta x_I + \beta u x_A \tag{1.29}$$

where x_R, x_A and x_I stand for **resting**, **activated** and **inhibited** microalgae photo states respectively and u stands for the local irradiance intensity. α,β,γ and δ describe the behavior of a particular strain under cultivation.

The actual growth rate is proportional to the spatial-averaged amount of activated state:

$$\mu = \kappa\gamma\overline{x_A} - M_e \tag{1.30}$$

Here M_e stands for metabolism overhead and κ is a constant of proportionality between the growth rate and averaged activated state amount for a particular strain.

In the scope of the presented papers, the PSF model was treated in a stochastic Lagrangian manner as expressed in figure 1.3.

It should also be noted, that the time-resolved Lagrangian models are definitely not a generally-valid answer to the microalgae growth modeling requirements. In the case of e.g. reactors with low cell density, short optical path and low sparge rates, especially in cases of the industrial scale outdoor photobioreactors is the use of models like PSF still unjustified because of the disproportionate increase of the computational costs. In such systems the mixing does not affect dramatically the resulting growth rate - see e.g. [64] and the growth models may be build on the assumption of the culture adopted to the average light intensity [10].

1.4 PBR modeling approaches

The problems enumerated in the preceding sections make it generally impossible to simulate the PBR directly without any simplification. If we are not capable yet of such a simulation, then we must strive to get so close as possible it. The following existing state-of-the-art solutions to the PBR simulation represent various degrees of such a simplification.

1.4.1 Scale-up methodology

This is an example of a simplification that can not be exploited in the case of the cultivation of the microalgae - as described further. The idea behind the scale-up methodology, as presented e.g. in [21, 70] on the case of the tubular photobioreactor, is very tempting from the computational point of view - to simulate only the small scale analogy of the production scale device, which is computationally much more feasible.

The basic principle is that an appropriate scale-up criterion is chosen, a one that ensures "equality" of the cultivation conditions between the small scale and production scale device. In the case of the photobioreactors, the light is the crucial and most influencing parameter, as already described earlier. In [21, 70] is thus a light related scale-up criterion chosen that leads to the same light/dark cycle frequency on all the scales.

This leads to the dependence of the axial fluid velocity on the bioreactor scale and as pointed out in [70] and further discussed in [34], such a scale-up approach thus has its natural limitations relevant to the hydrodynamic shear stress associated with the increase of the fluid flow velocity. As is also further discussed in [34], the frequency of the light/dark cycles is not a fully satisfying criterion not only because of the shear stress, but also because of the importance of the duty cycle.

1.4.2 Multizonal approach

The main reason for the current inability to directly simulate the production-scale bioreactor is that the full-scale CFD simulation coupled with the full-scale reaction simulation is still too computationally demanding. The first attempts to overcome this computational obstacle led to the oversimplified models based on the mixing idealization over the whole volume of the bioreactor, which make it impossible to correctly simulate the impact of the local hydrodynamic conditions (e.g. shear stresses) on the reaction model and vice-versa (e.g. the impact

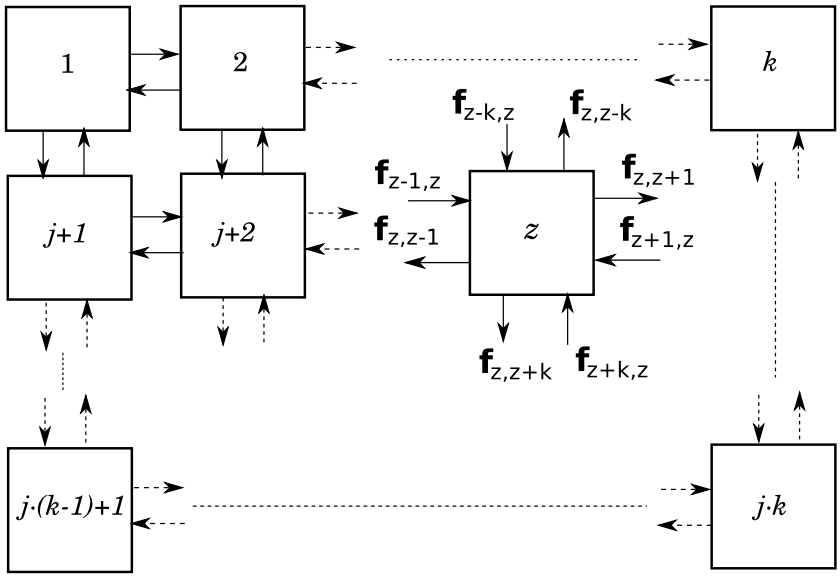

Figure 1.4: Two-dimensional schematic depiction of the multizonal model separating the simulated domain into a set of well mixed zones. The mass and energy transfer between the adjacent zones is captured by the vector $\mathbf{f}$.

of the inhomogeneous product concentration on the model of the transport). Subsequently the efforts to farther improve the accuracy of these models led to the so-called multizonal approach, which still avoids the full-scale CFD but improves the model accuracy by spatially splitting the simulated domain into a set of well-mixed zones. The advantage of the multizonal models is also that, while increasing the process simulation accuracy, they do not represent any major increase in the computational complexity. Figure 1.4 depicts schematically a 2 dimensional domain split into a set of zones. The mass and energy transfer between the adjacent zones is captured in the form of vector $\mathbf{f}$.

The multizonal approach has already been a research subject for several decades, as already the authors in e.g. [71, 72, 73] have used the method to model a stirred tank bioreactor. The weaknesses of the approach are the determination of the mass and energy transfer between the adjacent zones and also the necessity of the zone allocation reflecting the relevant transport and

reaction phenomena.

Attempts to further improve the multizonal model led subsequently to the development of the hybrid models - the multizonal/CFD models. See e.g. [74, 75, 76, 77] for a generalized framework for the multiscale modeling based on multizonal/CFD approach.

Authors in [46] have successfully employed the method to the simulation of the microalgae growth in the Couette-Taylor photobioreactor - with inter-compartment flows estimated by means of classical CFD.

1.4.3 Stochastic approach

Stochastic approaches to the PBR modeling try to express the hydrodynamic conditions inside the PBR in such a statistical form that would allow for the prediction of the irradiance history of the individual cells or their volumetric equivalents. The statistical approaches may be based either on the discretization of the simulated domain into a set of well-mixed/parameter-homogeneous zones where the statistical model yields the flux coefficients between the adjacent zones and the average cell residence time in each of the zones or on the random walk (RW) based simulation of transport by the turbulent diffusion, which is the subject of the subsequent text.

In [33] a dispersion coefficient dependent on both the spatial location and the "mixing force" (e.g. angular speed of rotational mixing or an average flow velocity caused by a pump) is used to evaluate the individual cell trajectories inside the PBR. Authors in [33] verify this approach on the case of a flat panel photobioreactor and come to the results consistent with classical methods - in this case the Finite Difference Method. In this Lagrangian approach, the individual cell trajectories through the simulated system are directly transformed into a stochastic description of the irradiance history - the timely course of the cell irradiance - which subsequently serves as a stochastic input variable to the ODE system of the reaction model (the Model of the Photosynthetic Factory in this case).

1.5 Computational performance

The PBR modeling simplification goes in the direction of decreasing the computational complexity of the simulated phenomena at the expense of the accuracy. But trying to find the alternative computational approaches to the models that are already available should not be underestimated. With the present day

technology and the growing availability of the massively parallel platforms, the potential hidden in the computational optimization may decrease the simulation times rapidly, while not compromising the accuracy of the relevant models.

With the emergence of the parallel platforms and parallel solvers, a question arises with respect to the suitability of the classical transport solving methods for these parallel platforms and implementations. While the classical methods, like e.g. the FVM method, are still of scientific interest with respect to its parallel implementation (see e.g. [78]), the fact, that these methods require too much information to be exchanged between the computational nodes leads to the search for an alternative transport solver with better properties regarding the parallel implementation.

The LBM method for the fluid flow offers an advantage over the classical CFD methods, like e.g. FVM, in the form of the perfectly local collision operator. It is also worth a note, that the LBM method stands on a solid grounds, because from the LBM model, the incompressible Navier-Stokes equations can be recovered - see e.g. [79] for further information.

In [36], the parallel potential of an alternative transport model based on the Lattice Boltzmann method for fluid flow simulation and its parallel performance are investigated. In the same paper the performance enhancement of the parallel stochastic implementation of the PSF-based reaction model is evaluated.

1.5.1 CUDA platform

CUDA (Compute Unified Device Architecture) emerged in 2006 as a result of the already present tendency to exploit the steadily increasing performance of the GPUs (Graphics Processing Unit) for the computationally intensive data processing - originally performed on CPUs (Central Processing Unit). While the CPUs are slowly adopting the parallel-core architectures, having several cores per single CPU, GPUs have typically hundreds or even thousands of parallel cores already. At the core of the CUDA platform are several key abstractions [80] - hierarchy of thread groups, shared memories and barrier synchronization. CUDA C - the platform programming language - is basically a minimal set of language extensions to the C programming language [80].

CUDA platform has already been employed for the parallel implementation of the Navier-Stokes CFD solver - see e.g. [81] as well as for the three dimensional parallel implementation of the Lattice Boltzmann method based flow solver, which has been presented in [82].

In my paper [36], CUDA-based performance enhancement to the LBM solver was evaluated based on the comparison between CPU implementation and

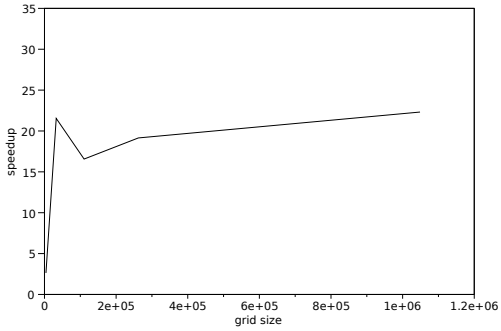

Figure 1.5: Performance comparison between GPU/CUDA-based LBM solver and CPU based solver. Computations were performed on AMD Athlon TM 64 X2 Dual Core Processor 5000+ and GeForce 9800 GT with 512 MB of memory.

CUDA implementation. Various grid sizes were evaluated and as depicted in figure 1.5, the speedup for the reasonably large grids was approximately 20.

Chapter 2

Papers

2.1 Paper I - Growth impact of hydrodynamic dispersion in a Couette-Taylor bioreactor

In this paper an extension of the lumped parameter model of the Photosynthetic Factory (PSF) into the domain with heterogeneously distributed parameters of irradiance and hydrodynamic dispersion is presented. The hydrodynamic dispersion based model is treated in the Eulerian manner in the form of differential model. The presented computational scheme is applied on the case of the Couette-Taylor photobioreactor (CTBR), where it is computationally evaluated using the finite difference scheme. Specifically for the case of the CTBR a simplification of the solution is proposed based on the axisymmetry and subsequent problem reduction from three-dimensional to one-dimensional space, where the one dimensional problem is aligned with the radial linear profile in the cylindrical gap of CTBR. The paper also shows that the hydrodynamic dispersion based model exhibits the limit growth rate reached by increasing the driving force expressed by the increasing parameters of the relevant hydrodynamic dispersion function, in this paper proposed in the following form:

$$D(x) = D_0(\omega)(p_0 + p_1[1 - (|2x - 1|)^n]) \tag{2.1}$$

In this equation $D(x)$ stands for the spatially dependent dispersion coefficient, $D_0(\omega)$ expresses the dependence of the dispersion profile along the radial

dimension x on the driving force - angular velocity ω of the inner cylinder. p_0, p_1 and n are dimensionless constants determined empirically.

The importance of the paper is also in the validation of the hydrodynamic dispersion based photobioreactor modeling, which is important for the possibility of employing the Lagrangian random walk based modeling approaches investigated in the subsequent paper.

Growth impact of hydrodynamic dispersion in Couette-Taylor bioreactor[☆]

Štěpán Papáček[a], Václav Štumbauer[a], Dalibor Štys[a], Karel Petera[b], Ctirad Matonoha[c]

[a] *Institute of Physical Biology, University of South Bohemia, 373 33 Nové Hrady, Czech Republic*
[b] *Czech Technical University in Prague, Faculty of Mechanical Engineering, Technická 4, 166 07 Praha 6, Czech Republic*
[c] *Institute of Computer Science, Academy of Sciences of the Czech Republic, Pod Vodarenskou vezi 2, 182 07 Prague 8, Czech Republic*

Abstract

The development of a distributed parameter model of microalgae growth is presented. Two modelling frameworks for photo-bioreactor modelling, Eulerian and Lagrangian, are discussed and the complications residing in the multi-scale nature of transport and reaction phenomena are clarified. It is shown why is the mechanistic two time-scale model of photosynthetic factory the adequate model for biotechnological purposes. For a special laboratory Couette-Taylor bioreactor with cylindrical geometry, we reached a reliable simulation results using steady-state Eulerian approach and the finite difference scheme. Moreover, we prove numerically that the resulting photosynthetic production rate in this reactor goes, for growing inner cylinder angular velocity, to a certain limit value, which depends on the average irradiance only.

Keywords: multi-scale modelling, distributed parameter system, boundary value problem, random walk, photosynthetic factory
PACS: 93C10, 37N25

1. Introduction

Biotechnology with microalgae and photo-bioreactor (PBR) design is nowadays regaining attention thanks to emerging projects of CO_2 sequestration and algae biofuels. Nevertheless, there neither exist reliable methods nor software for modelling, simulation and control of PBR [14]. Modelling in a predictive way

[☆]This work was supported by the grants MŠMT MSM 600 766 58 08, and the institutional research plan No. AV0Z10300504.

Email addresses: papacek@alga.cz (Štěpán Papáček), stumbav@gmail.com (Václav Štumbauer), stys@jcu.cz (Dalibor Štys), karel.petera@fs.cvut.cz (Karel Petera), matonoha@cs.cas.cz (Ctirad Matonoha)

the photosynthetic response in the three-dimensional flow field seems unrealistic today, because the global response depends on numerous interacting intracellular reactions, with various time-scales. In our previous works [10, 13, 11], we examined an adequate multi-scale lumped parameter model, describing well the principal physiological mechanisms in microalgae: photosynthetic light-dark reactions and photoinhibition. Now our main goal is the development and implementation of a mathematical model of microalgae growth in a general gas-liquid-solid PBR as tool in PBR design and optimization of its performance. Afterward, as a case study, we simulate the growth of microalgae in Couette-Taylor bioreactor [9], in order to validate our results.

2. Development of a distributed parameter model of microalgae growth in a PBR

Leaving apart the inherently non-reliable scale-up methodology for PBR design [14], two main approaches for transport and bioreaction processes modelling are usually chosen [15]: (i) Eulerian, and (ii) Lagrangian. While the Eulerian approach, resulting in partial differential equations, is a usual way to describe transport and reaction phenomena in bioreactors, the Lagrangian approach, leading either to stochastic ordinary differential equations or to random walk simulation of transport by turbulent diffusion (hydrodynamic dispersion), is an interesting alternative to PBR models.

Till nowadays, the most important information about the photosynthetic production of some microalgae species resides in the measurement of the coupling between photosynthesis and irradiance (being a controlled input), in form of the steady-state light response curve (so-called *P–I curve*), which represents the microbial kinetics, see e.g. *Monod* or more general *Haldane* type kinetics [15]. However, PBR operating under high irradiance, permitting large non-homogeneities of irradiance and allowing the photoinhibition of the cell culture and the photolimitation as well, belong to intensively studied topics of microalgal biotechnology, see e.g. [14] and references within there. Hence, we need such a model of microalgal growth, which can describe both the steady state and dynamic phenomena, i.e. it has to fulfill the following experimental observations: (i) the steady state kinetics is of *Haldane* type or *Substrate inhibition kinetics* [8]; (ii) the microalgal culture in suspension has the so-called *light integration* property [16, 8], i.e. as the light/dark cycle frequency is going to infinity, the value of the resulting production rate (e.g. oxygen evolution rate) goes to a certain limit value, which depends on the average irradiance only [10]. These features are best comprised by the mechanistic **model of photosynthetic factory** - PSF model [6, 17, 10]. Using the re-parametrization firstly introduced in [13], three-state PSF model has the following form:

$$\dot{y} = \big[\mathcal{A} + u(t)\mathcal{B}\big]y, \qquad \mu = q_2 q_3 (1+q_5)\; y_A(t)\;, \tag{1}$$

$$\mathcal{A} = q_4 \begin{bmatrix} 0 & q_2(1+q_5) & \frac{q_5}{q_2(1+q_5)} \\ 0 & -q_2(1+q_5) & 0 \\ 0 & 0 & -\frac{q_5}{q_2(1+q_5)} \end{bmatrix}, \quad \mathcal{B} = q_4 \begin{bmatrix} -1 & 0 & 0 \\ 1 & -q_5 & 0 \\ 0 & q_5 & 0 \end{bmatrix}, \tag{2}$$

where $y = (y_R, y_A, y_B)^\top$, $y_R + y_A + y_B = 1$, and $q_i,\ i = 1..5$, are five positive model parameters, cf. [13, 11]. Notice that (1) is composed by one ODE system and one algebraic equation connecting the hypothetical state y_A of PSF model with the specific growth rate $\mu := \dot{c_x}/c_x$, where c_x stands for microbial cell concentration. Considering that the values of q_3 in s^{-1} and q_5 (dimensionless) are of order 10^{-4}, cf. [17, 13, 11], and $y_A(t)$ is periodic with period T, cf. [10] for more details, we have for the specific growth rate: $\mu = \frac{q_2 q_3 (1+q_5)}{T} \int_0^T y_A(t)\mathrm{d}t$, and we see that PSF model successfully simulates the growth in high-frequency fluctuating light conditions because the growth is described through the "fast" state y_A. Hence the sensitivity to high-frequency inputs, see e.g. flashing light experiments [8] or light/dark cycles induced by hydrodynamic mixing, is reached. The single scalar input $u(t)$, representing the dimensionless irradiance in the culture, is defined as $u := I/q_1$, where I is the non-scaled irradiance (units: μE m^{-2} s^{-1}), and $q_1 := I_{opt}$ (I_{opt} maximizes μ). It is assumed that $u(t)$ is at least piecewise continuous. In other words, PSF model is the so-called bilinear controlled system which inherent property is the so-called light integration capacity [8], i.e. due to the *Lipschitz dependence of trajectories on control*, cf. [3] and references within there, as the frequency of fluctuating light is going to infinity, the value of resulting production rate (specific growth rate μ) goes to a certain limit value, which depends on average irradiance only [10]. For the constant input signal (irradiance $u \geq 0$) the ODE system (1) is linear and its system matrix $\mathcal{A} + u\mathcal{B}$ has three distinct eigenvalues. Two eigenvalues are negative ($\lambda_F,\ \lambda_S$), and the third is zero (its corresponding eigenvector is the globally stable steady state solution of (1)). In the sequel, we will need the steady state values of states y_A and y_B: $y_{A\,ss} = \frac{u}{q_2(1+q_5)(u^2+u/q_2+1)}$, $\quad y_{B\,ss} = \frac{u^2}{u^2+u/q_2+1}$.

Finally we can see that the steady state PSF model behavior is defined by the parameters q_1, q_2, q_3, and the PSF model dynamics is determined by the *fast* rate q_4 and the *slow* rate $q_4 q_5$, for more details cf. [13, 11].

Eq. (1) represents, for some known input signal $u(t)$, the **Lagrangian model of PBR**. However, it should be stressed that $u(t)$ is a random variable, depending on the fluid flow in PBR.

In some special, although common, conditions, e.g. in the case of constant average irradiance $u_{av} := \frac{1}{t_f - t_0} \int_{t_0}^{t_f} u(t)\mathrm{d}t$, and when the period of light fluctuation is "small", we can simplify the ODE system (1) by reducing the PSF model dynamics to the one dimensional system using the singular perturbation approach with respect to the small parameter $q_5 \approx 10^{-4}$. The system (1) thanks to the properties of its right hand side clearly satisfies the sufficient condition for the convergence of the singular perturbation [7]. One can therefore take the limit $q_5 \to 0$ in (1) to obtain:[1] $\dot{y_A}^F = -q_4 q_2\ {y_A}^F + q_4 u(t)\ y_R$, $\dot{y}_B^F = 0$, and

[1] Roughly speaking we can also apply the theorem of *Lipschitz dependence of trajectories on control* [3, 10, 11] when we suppose that the period of light cycles is "sufficiently small" for "averaging" of y_B but not so small for averaging y_A.

consequently (recall that $y_R = 1 - [y_A + y_B]$):

$$\dot{y_A}^F = -q_4(u(t) + q_2){y_A}^F + q_4 u(t)\left[1 - y_{B\,ss}\left(u_{av}\right)\right] \ . \tag{3}$$

3. Microalgae growth in Couette-Taylor bioreactor: Simulation results

We aim to simulate, eventually to optimize, microalgae cell growth in a Couette-Taylor bioreactor (CTBR) with cylindrical geometry, cf. [9]. For the sake of clarity, we further suppose all phenomena are axi-symmetrical, i.e. CTBR is homogeneously illuminated from the outside, and the biomass concentration is sufficiently high for making irradiance level decreasing from the CTBR outer wall to the CTBR core. Thus, the CTBR volume (our computational domain) can be divided into layers with the same irradiance level. Moreover, we also transform the 3D fluid dynamics problem into the one-dimensional. It means that only the cell motion in direction of light gradient is taken into account. Let then suppose this motion is caused by the turbulent diffusion (hydrodynamic dispersion) characterized by the dispersion coefficient $D_e(r)$, the tensor of second order in 3D case.

As stated before, the only input parameter determining the bio-reaction rate is the spatially dependent irradiance $u(r)$. Based on [5] we use the following relations for $u(r)$ and for the average (absorbed) irradiance:

$$u(r) = \frac{R\ u_1}{r}\frac{\cosh\kappa\frac{r}{R}}{\sinh\kappa}\ ,\ u_{av} = u_1\frac{2R^2}{R^2 - {r_0}^2}\frac{[\sinh\kappa - \sinh\kappa\frac{r}{R}]}{\kappa\cosh\kappa}\ , \tag{4}$$

where u_1 is the incident irradiance on the outer CTBR wall, κ is the dimensionless attenuation coefficient, R and r_0 are the outer and inner cylinder radii, respectively. The dimensionless attenuation coefficient $\kappa > 0$ is defined as follows: $\kappa := \frac{\ln(2)R}{r_{1/2}}$, where $r_{1/2}$, is the length interval (unit: m) making diminish the intensity of light to one half (in rectangular geometry). Furthermore, we introduce the dimensionless spatial coordinate in radial direction x, and dimensionless dispersion coefficient $p(x)$ as follows:

$$x := \frac{r}{R},\ x \in [\frac{r_0}{R}, 1], D_e := p(x)\ D_0,\ p(x) := p_0 + p_1\left[1 - \left(|2x - 1|\right)^n\right], \tag{5}$$

where D_0 is a constant with some characteristic value (unit: $\mathrm{m^2 s^{-1}}$), and p_0, p_1, n are dimensionless positive constants (to be determined empirically).

According to [2], nearly all mass transfer is linearly dependent on the driving force. Hence, for the growing power supply to the CTBR (by augmenting inner cylinder angular velocity ω) we expect D_0 proportionally grows, meanwhile the D_e shape, i.e. $p(x)$, remains constant.

All the values needed to perform further calculations are summarized in Table 1 (u_1 is chosen accordingly to fulfill the condition $u_{av} = 1$):

Similarly as in our work [12], Lagrangian time dependent simulation (data not shown) revealed that the state vector converges to a steady state in few minutes (this is the time scale of the photoinhibition process). Moreover, only the

u_1	D_0	κ	r_0	R	p_0	p_1	q_2	q_4	n
$\frac{R^2-{r_0}^2}{2R^2}\frac{\kappa\cosh\kappa}{[\sinh\kappa-\sinh\kappa\frac{r}{R}]}$	0.0001	$24\ln(2)$	0.04	0.06	2	1	0.3	0.5	2

long term cultivation either in continuous or batch operation mode, where the quasi-steady state is reached, is of biotechnological importance. Consequently, based on the above reasons, our **Eulerian modelling approach** is simpler than generally three dimensional non-stationary transport-reaction PDE system: $\frac{\partial y}{\partial t} - \nabla\cdot(D_e(\vec{r})\nabla y) = \big[\mathcal{A} + u(r)\mathcal{B}\big]y$ in $\Omega, \nabla y = 0$ on $\partial\Omega$. Furthermore, employing the fast reduction (3) and omitting the upper index "F",[2] we get only one ODE for modelling the steady state of one state y_A in radial direction x (i.e. x is the only one independent variable):

$$-\frac{1}{x}\left[xp(x)y_A'\right]' + q(x)\ y_A = q(x)\ y_{A_\infty},\quad y_A'(r_0/R) = 0,\ y_A'(1) = 0\ , \qquad (6)$$

where $q(x) := \frac{q_4(u(x)+q_2)\ R^2}{D_0}$. The function $y_{A_\infty}(x)$ is calculated as the steady state solution of (3):

$$y_{A_\infty}(x) = \frac{u(x)}{u(x)+q_2}\left[1 - y_{B_{ss}}(u_{av})\right] = \frac{u(x)}{u(x)+q_2}\left[\frac{u_{av}+q_2}{q_2({u_{av}}^2 + u_{av}/q_2 + 1)}\right].$$

Let be defined the characteristic number, the so-called *Damköhler number* of second type, as $Da_{II} := \frac{q_4\ R^2}{D_0}$, then $q(x) := (u(x)+q_2)\ Da_{II}$ holds. In the sequel, the dependence of the solution of (6) on Da_{II} will be studied.

The **boundary value problem** with Neumann boundary conditions and inhomogeneous right-hand side (6) has a lot of nice properties. It is symmetric and positive and the corresponding linear differential operator of the second order is self-adjoint. As $q(x) > 0$, problem (6) has a unique solution. It was solved numerically using the finite difference scheme for uniformly distributed nodes with the steplength h, cf. [1]. It leads to the symmetric and positive definite system of linear equations with the tridiagonal matrix for unknown values

$$y_{A_i} = y_A(x_i) \equiv y_A(x_i, \infty), \quad i = 0, \ldots, N.$$

The scheme approximates the exact solution of the boundary value problem (6) with accuracy of order h^2.

In our numerical experiments we have chosen the values from Table 1 together with $N = 1000$. The following Fig. 1 shows the dependence of the solution on the *Damköhler number* Da_{II}. We can see that the solution approaches constant value $y_A(x,\infty) = 0.625$ for $Da_{II} \to 0$. Let us see that the solution becomes flatter for decreasing Da_{II} and for $Da_{II} = 0.1$ the solution is nearly constant. Notice also that the value $y_A = 0.625$ corresponds to the value $y_{A_{ss}}(1) = \frac{1}{2q_2+1}$,

[2]The lower index "ss" is omitted as well, nevertheless, when some confusion could arise, the term $y_A(x,\infty)$ is used.

cf. (2). This means that the ODE system (6), for the case $Da_{II} \to 0$, performs the "averaging" of $u(x)$.

From practical point of view, in order to maximize the specific growth rate, cf. (1), it is important to evaluate the integral average of the activated state $y_A(x, \infty)$, depending on the operational conditions, i.e. on the u_1 and on ω. Let define

$$J = \frac{1}{V} \int_V y_A(x, \infty) \mathrm{d}V = \frac{2}{R^2 - {r_0}^2} \int_{r_0/R}^{1} x y_A(x, \infty) \mathrm{d}x \ , \tag{7}$$

recalling that $y_A(x, \infty)$ is a solution of (6). Then we can formulate the optimization problem residing in maximizing of J. The next Fig. 2 shows the dependence of J, cf. (7), on Da_{II}, for the incident irradiance u_1 taken from Table 1. The maximum value arises for $Da_{II} \to 0$ and its value is again $J = 0.625$. The minimum value in (7) arises when the solution of (6) is $y_A(x, \infty) = y_{A_\infty}(x)$, which leads to a value $J \approx 0.4539$.

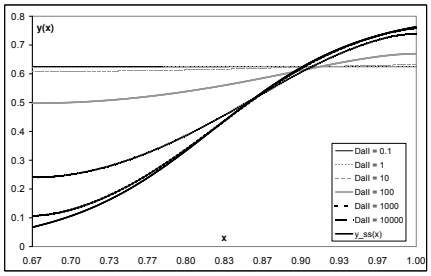

Fig. 1. Approximate solution of (6): $y_A(x, \infty)$ vs. x.

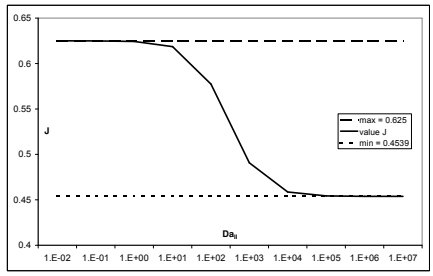

Fig. 2. Performance index J, cf. (7), vs. Da_{II}.

4. Conclusions

The main benefit of this paper resides in an extension of a multi-scale lumped parameter model of photosynthetic factory to the domain with heterogeneously distributed relevant parameters; in our case these parameters are irradiance and hydrodynamic dispersion (turbulent diffusion). For a special laboratory bioreactor based on Couette-Taylor flow, the so-called Couette-Taylor bioreactor, we reached reliable simulation results using Eulerian modelling framework and the finite difference scheme. Moreover, our results reflect well the dependence of microalgae growth on *Damköhler number* Da_{II}, i.e. on hydrodynamic dispersion (depending on inner cylinder angular velocity ω), permitting the announcement of our statement about *light integration property of PSF model* for CTBR as well: The resulting photosynthetic production rate in CTBR, for growing ω, goes to a certain limit value, which depends on the average irradiance only.

References

[1] Babuška I., Práger M., Vitásek E.: *Numerical Processes in Differential Equations*, John Wiley & Sons, London, 1966.

[2] Beek W.J., Muttzall K.M.K., van Heuven J.W.: *Transport Phenomena*, Wiley & Sons, 2000.

[3] Čelikovský S.: On the continuous dependence of trajectories of bilinear systems on controls and its applications. *Kybernetika*, 24 (1988), 278–292.

[4] Čelikovský S., Papáček Š., Cervantes-Herrera A., and Ruiz-León J.: Singular Perturbation Based Solution to Optimal Microalgal Growth Problem and its Infinite Time Horizon Analysis. *TAC IEEE*, 55 (3): 767–772, 2010.

[5] Cornet J.-F., Dussap C. G., Gros J.-B., Binois C., Lasseur C.: A simplified monodimensional approach for modeling coupling between radiant light transfer and growth kinetics in photobioreactors. *Chemical Engineering Science*, 50 (1995), 1489–1500.

[6] Eilers, P.H.C., Peeters, J.C.H.: Dynamic behaviour of a model for photosynthesis and photoinhibition. *Ecological Modelling*, 69 (1993), 113–133.

[7] H. K. Khalil: Perturbation and averaging. In *Nonlinear systems*, Prentice Hall, 2002.

[8] Nedbal L., Tichý V., Xiong F., Grobbelaar J.U.: Microscopic green algae and cyanobacteria in high-frequency intermittent light. *J. Appl. Phycol.*, 8 (1996), 325–333.

[9] Papáček Š., Štys D., Dolínek P., Petera K.: Multicompartment/CFD modelling of transport and reaction processes in Couette-Taylor photobioreactor. *Applied and Computational Mechanics*, 1 (2007), 577–586.

[10] Papáček Š., Čelikovský S., Štys D., Ruiz-León J. : Bilinear System as Modelling Framework for Analysis of Microalgal Growth. *Kybernetika*, vol. 43 (2007), 1–20.

[11] Papáček Š., Čelikovský S., Rehák B., Štys D.: Experimental design for parameter estimation of two time-scale model of photosynthesis and photoinhibition in microalgae. *Math. Comput. Simul.*, 80 (2010), 1302–1309.

[12] Papáček Š., Matonoha C., Štumbauer V., Štys D.: Modelling and simulation of photosynthetic microorganism growth: Random walk vs. Finite difference method. Submitted to *Math. Comput. Simul.*, Special Issue: Modelling 2009.

[13] Rehák, B., Čelikovský S., Papáček, Š.: Model for Photosynthesis and Photoinhibition: Parameter Identification Based on the Harmonic Irradiation O_2 Response Measurement. Joint Special Issue of *TAC IEEE* and *TCAS IEEE*, (2008), 101–108.

[14] Richmond, A.: Biological Principles of Mass Cultivation. In: *Handbook of Microalgal Culture: Biotechnology and Applied Phycology*, A. Richmond, Ed., Blackwell Publishing (2004), 125–177.

[15] Schugerl K., Bellgardt K.-H. (Eds): *Bioreaction Engineering, Modeling and Control.* Springer-Verlag, Berlin, Heidelberg, 2000.

[16] Terry K. L.: Photosynthesis in Modulated Light: Quantitative Dependence of Photosynthetic Enhancement on Flashing Rate. *Biotechnology and Bioengineering*, 28 (1986), 988–995.

[17] Wu X., Merchuk J.C.: A model integrating fluid dynamics in photosynthesis and photoinhibition processes. *Chemical Engineering Science*, 56 (2001), 3527–3538.

2.2 Paper II - Modelling and simulation of photosynthetic microorganism growth: random walk vs. finite difference method

In this paper two different PBR modeling approaches are compared to each other, namely the Eulerian Finite difference based approach and Lagrangian Random Walk (RW) based approach. By the successful comparison, the validity of the RW method is proven. The comparison is based on the PBR productivity devised from the model of Photosynthetic Factory (PSF) - specifically on the timely-averaged steady-state amount of the PSF activated state y_a to which the PBR productivity is directly proportional. The steady-state timely-averaged amount of y_a reached under optimal operating conditions was 0.62 for the RW based method and 0.625 for the finite difference based method.

Further it was shown, that the Lagrangian RW based method allows the massively parallel implementation - the possible performance enhancement was studied between the single threaded RW based implementation on the classical (CPU AMD AthlonTM 64 X2 Dual Core Processor 5000+) and a parallel implementation on the Compute Unified Device Architecture (CUDA), which was evaluated on GeForce 9800 GT with 512 MB of memory. Despite the slight difference in the random number generator implementations (RNG) given by the different library RNG implementations on CUDA and Boost, the CUDA based implementation has been shown to be 90 times faster.

Modelling and simulation of photosynthetic microorganism growth: Random walk vs. Finite difference method[☆]

Štěpán Papáček[a], Ctirad Matonoha[b], Václav Štumbauer[a], Dalibor Štys[a]

[a] *Institute of Physical Biology, University of South Bohemia, 373 33 Nové Hrady, Czech Republic*
[b] *Institute of Computer Science, Academy of Sciences of the Czech Republic, Pod Vodarenskou vezi 2, 182 07 Prague 8, Czech Republic*

Abstract

The paper deals with photosynthetic microorganism growth modelling and simulation in a distributed parameter system. Main result concerns the development and comparison of two modelling frameworks for photo-bioreactor modelling. The first "classical" approach is based on PDE (reaction-turbulent diffusion system) and finite difference method. The alternative approach is based on random walk model of transport by turbulent diffusion. The complications residing in modelling of multi-scale transport and reaction phenomena in microalgae are clarified and the solution is chosen. It consists on phenomenological state description of microbial culture by the lumped parameter model of photosynthetic factory (PSF model) in the re-parametrized form, published recently in this journal by Papáček, et al. (2010). Obviously both approaches lead to the same simulation results, nevertheless they provide different advantages.

Keywords: multi-scale modelling, distributed parameter system, boundary value problem, random walk, photosynthetic factory
PACS: 93C10, 37N25

1. Introduction

The photosynthetic microorganism growth description is usually based on the microbial kinetics (so-called *P–I curve*), i.e. on the static lumped parameter models (LPM) describing the photosynthetic response in small cultivation

[☆]This work was supported and co-financed by the South Bohemian Research Center of Aquaculture and Biodiversity of Hydrocenoses (CZ.1.05/2.1.00/01.0024) by the grant MŠMT MSM 600 766 58 08, the South Bohemia University grant GA JU 152//2010/Z, and the institutional research plan No. AV0Z10300504.

Email addresses: papacek@alga.cz (Štěpán Papáček), matonoha@cs.cas.cz (Ctirad Matonoha), stumbav@gmail.com (Václav Štumbauer), stys@jcu.cz (Dalibor Štys)

systems with a homogeneous light distribution [5, 21]. However, there is an important phenomenon, which occurs under fluctuating light condition, the so-called flashing light enhancement, demanding some other model than it residing in the artificial connection between the steady state kinetic model and the empiric one describing the photosynthetic productivity under fluctuating light condition, see e.g. [22]. Nevertheless, even having an adequate dynamical LPM of microorganism growth, e.g. phenomenological model of so-called photosynthetic factory [6, 7, 9, 25], another serious difficulty resides in the description of the microalgal growth in a photo-bioreactor, i.e. in a distributed parameter system with strongly non-homogeneous light distribution, e.g. accordingly to the exponential attenuation, see Section 4.

In our previous papers [15, 19, 17, 16, 4] we studied the PSF model behavior and the techniques for parameter estimation as well. In this paper we aim to develop the distributed parameter model (DPM) of a photosynthetic microorganism growth in a photo-bioreactor (PBR), mainly due to the necessity to evaluate the PBR performance and to optimize PBR operating conditions. Leaving apart the inherently non-reliable scale-up methodology for PBR design [8, 12], two main approaches for transport and bioreaction processes modelling are usually chosen [21]: (i) Eulerian, and (ii) Lagrangian. While the Eulerian approach, leading to the partial differential equations (PDE), is an usual way to describe transport and reaction systems, the Lagrangian approach, resulting either in a stochastic ordinary differential equations, or in the further described technique based on random walk simulation of transport by turbulent diffusion, is an interesting alternative to the PDE models.

The main purpose of this paper is to clarify how the PSF model can be advantageously used in DPM of microalgae growth in a general PBR. Hence, after having presented the main results concerning PSF model as LPM in Section 2, in Section 3 we present the development of two above mentioned modelling approaches. Section 4 is devoted to simulate PBR performance. As a case study we took the PBR with rectangular geometry, see e.g. the flat-panel PBR and FMT 150 in Fig. 1 (for more details cf. [11] and references within there), receiving the problem depending only on one space coordinate in direction of light gradient. This simplification permits to formulate the simple optimization problem, having as result the incident irradiance maximizing the PBR productivity (Subsection 4.3). The simulation results and advantages of each approach, as well as outlooks for further research, are discussed in the final section.

2. Lumped parameter model of photosynthesis and photoinhibition in microalgae

The dynamical **model of photosynthetic factory – PSF model**, see Fig. 2 below, has been thoroughly studied in the biotechnological literature [6, 7, 9, 25]. The state vector y of the PSF model is three dimensional, namely, $y = (y_R, y_A, y_B)^\top$, where y_R represents the probability that PSF is in the resting state R, y_A the probability that PSF is in the activated state A, and y_B the

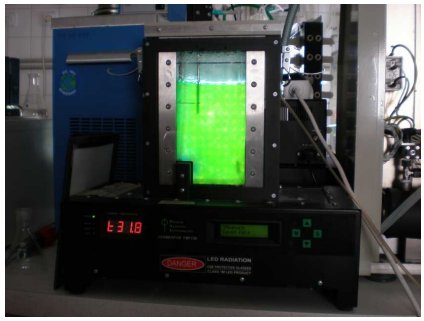
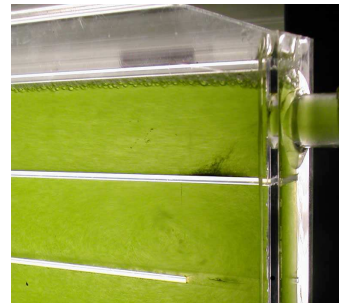

Figure 1: Two examples of rectangular PBR geometry: Photobioreactor FMT 150, made by Photon Systems Instruments, Czech Republic, www.psi.cz (left), and Flat panel photobioreactor, Institute of Physical Biology, University of South Bohemia, Nové Hrady, Czech Republic (right).

probability that PSF is in the inhibited state B. The PSF can only be in one of these states, so:

$$y_R + y_A + y_B = 1 \ . \tag{1}$$

The PSF model has to be completed by an equation connecting the hypothetical states of PSF model with some quantity related to the cell growth. This quantity is the specific growth rate μ.[1] According to [6, 25], the rate of photosynthetic production is proportional to the number of transitions from the activated to the resting state, i.e. $\gamma\ y_A(t)$. Hence, for the average specific growth rate we have the relation:

$$\mu = \frac{\kappa\gamma}{t_f - t_0} \int_{t_0}^{t_f} y_A(t)\mathrm{d}t \ , \tag{2}$$

where κ is a new dimensionless constant – the fifth PSF model parameter. Equation (2) reveals the reason why PSF model can successfully simulate the microalgae growth in high-frequency fluctuating light conditions: the growth is described through the "fast" state y_A, hence the sensitivity to high-frequency input fluctuations is reached, see e.g. flashing light experiments [14].

2.1. Re-parametrization of the PSF model

Using the re-parametrization firstly introduced in [19], PSF model has the following form (recall that $y = (y_R, y_A, y_B)^\top$):

$$\dot{y} = \big[\mathcal{A} + u(t)\mathcal{B}\big]y, \tag{3}$$

$$\mathcal{A} = q_4 \begin{bmatrix} 0 & q_2(1+q_5) & \frac{q_5}{q_2(1+q_5)} \\ 0 & -q_2(1+q_5) & 0 \\ 0 & 0 & -\frac{q_5}{q_2(1+q_5)} \end{bmatrix}, \quad \mathcal{B} = q_4 \begin{bmatrix} -1 & 0 & 0 \\ 1 & -q_5 & 0 \\ 0 & q_5 & 0 \end{bmatrix}, \tag{4}$$

[1] $\mu := \dot{c}/c$, where c is the microbial cell density. The notation used is the most usual in biotechnological literature, cf. [5].

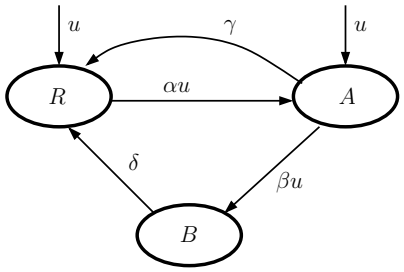

Figure 2: States and transition rates of the photosynthetic factory – Eilers and Peeters's PSF model.

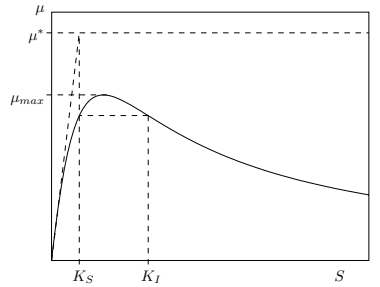

Figure 3: Steady-state production curve of *Haldane* type or *Substrate inhibition kinetics*. S stands here for irradiance.

where the new parameters $q_i,\ i = 1, .., 5$, are related to the old ones as follows:

$$q_1 := \sqrt{\frac{\gamma\delta}{\alpha\beta}},\ q_2 := \sqrt{\frac{\alpha\beta\gamma}{\delta(\alpha+\beta)^2}},\ q_3 := \kappa\gamma\sqrt{\frac{\alpha\delta}{\beta\gamma}},\ q_4 := \alpha q_1,\ q_5 := \beta/\alpha. \quad (5)$$

The single scalar input $u(t)$, representing the dimensionless irradiance in the culture, is defined as $u := I/q_1$, where I is the non-scaled irradiance (units: μE m^{-2} s^{-1}). It is assumed that $u(t)$ is at least piecewise continuous. In other words, PSF model is the so-called bilinear controlled system which inherent property is the so-called light integration capacity [14], i.e. due to the *Lipschitz dependence of trajectories on control*, cf. [3] and references within there, as the frequency of fluctuating light is going to infinity, the value of resulting production rate (specific growth rate μ) goes to a certain limit value, which depend on average irradiance only [15].

Let see that $q_1 = I_{opt}$ (I_{opt} maximizes μ, see Fig. 3 and Remark 1), $q_2,\ q_5$ are dimensionless, $q_3,\ q_4$ are in s^{-1}. The reasoning for such a choices arises from the utility to separate the steady state PSF model behavior (parameters q_1, q_2, q_3) from the PSF model dynamics (the *fast* rate $q_4 := \alpha I_{opt}$ and the *slow* rate $q_4 q_5 := \beta I_{opt}$), for more details cf. [19, 17]. The relation for the specific growth rate is now:

$$\mu = q_2 q_3 (1 + q_5) \frac{1}{t_f - t_0} \int_{t_0}^{t_f} y_A(t)\mathrm{d}t\ . \quad (6)$$

For the constant input signal (irradiance $u \geq 0$) the ODE system (3) is linear and its system matrix $\mathcal{A} + u\mathcal{B}$ has three distinct eigenvalues. Two eigenvalues are negative ($\lambda_F,\ \lambda_S$), and the third is zero (its corresponding eigenvector is the globally stable steady state solution of (3)). In the sequel, we will need the steady state values of states y_A and y_B:

$$y_{A_{ss}} = \frac{u}{q_2(1+q_5)(u^2 + u/q_2 + 1)}\ , \quad y_{B_{ss}} = \frac{u^2}{u^2 + u/q_2 + 1}\ . \quad (7)$$

Remark 1: Notice that the parameter q_5 quantifies the separation between the fast and slow dynamic; $q_5 \approx 10^{-4}$, based on [25].[2] Moreover, the PSF model steady state behavior corresponds to *Haldane* type kinetics (or so-called *Substrate inhibition kinetics*), see Fig. 3: $\mu = \frac{\mu^* \ I}{K_S + I + I^2/K_I}$, where I is irradiance (i.e. limiting substrate S for photosynthetic microorganism) and μ^*, K_S, K_I are model constants. The connection between PSF model and *Haldane kinetics* could be described as follows: $\mu^* = q_2 q_3$, $K_S = q_1 q_2$, and $K_I = \frac{q_1}{q_2}$. For the constant value of irradiance which maximizes the steady-state growth rate, i.e. $I_{opt} := q_1 = \sqrt{K_S K_I}$, holds $\mu(I_{opt}) := \mu_{max} = \frac{\mu^*}{2\sqrt{K_S/K_I}+1} = \frac{q_2 q_3}{2q_2+1}$. See also that for $K_I \to \infty$, the production curve changes to *Monod* kinetics.

2.2. Order reduction of the ODE system (3)

In some special although common conditions, e.g. in the case of constant average irradiance $u_{av} := \frac{1}{t_f - t_0} \int_{t_0}^{t_f} u(t)\mathrm{d}t$, and when the period of light fluctuation is "small", we can simplify the ODE system (3) by reducing the PSF model dynamics to the one dimensional one using the singular perturbation approach with respect to the small parameter $q_5 \approx 10^{-4}$ [23]. The system (3) thanks to the properties of its right hand side clearly satisfies the sufficient condition for the convergence of the singular perturbation. One can therefore take the limit $q_5 \to 0$ in (3) to obtain

$$\dot{y_A}^F = -q_4 q_2 \ {y_A}^F + q_4 u(t) \ y_R \ , \ \dot{y}_B^F = 0 \ . \tag{8}$$

Upper index "F" aims to avoid confusion with notation for the non-reduced model (3). Taking into account the normalization condition (1), and preferring the states y_A, y_B (due to their measurability[3]), we further analyze only two above differential equations (8); for more detail see our paper [17]. The second relation in (8), i.e. $\dot{y}_B^F = 0$, means that the "slow" state variables reach its steady state value, i.e., $y_B = y_{B_{ss}}(u_{av})$. Recalling relation (1), i.e., $y_R = 1 - y_A - y_B$, only one ODE for the fast dynamics of ${y_A}^F$ state is received:

$$\dot{y_A}^F = -q_4(u(t) + q_2){y_A}^F + q_4 u(t) \left[1 - y_{B_{ss}}(u_{av})\right] \ . \tag{9}$$

Roughly speaking we can also apply the theorem of *Lipschitz dependence of trajectories on control* [3, 15, 17] when we suppose that the period of light cycles is "sufficiently small" for "averaging" of y_B but not so small for averaging y_A. Further we denote the steady state solution of the above equation (9) as: y_{A_∞}. In subsection 4.3, we shall advantageously use this term.

[2] For the microalga *Porphyridium* sp., on basis of Wu and Merchuk's parameters α, β, γ, δ, κ, we have calculated: $q_1 = 250.106$ μE m^{-2}, $q_2 = 0.301591$, $q_3 = 0.176498e-3$ s^{-1}, $q_4 = 0.483955$ s^{-1}, $q_5 = 0.298966e-3$.

[3] The connection of y_A with a measurable quantity describes (6), and y_B can be estimated via chlorophyll fluorescence measurement, cf. [11, 25].

3. Distributed parameter model of photosynthesis and photoinhibition in microalgae

Two approaches for modelling of microbial growth are usually chosen: (i) Eulerian, and (ii) Lagrangian. The first "more classical" approach, based on the balance equation for an infinitesimal volume, leads to the partial differential equation (reaction-convection-diffusion system). The quantities to describe are concentrations of microbial cells and some other species.

The Lagrangian approach, consisting in description of each individual microbial cell, offers two possibilities: first, to compute or measure (cf. e.g. [10]) the cell trajectories in PBR and evaluate the so-called irradiance history $u(t)$ as the stochastic input variable for the ODE (3), resulting in a stochastic ordinary differential equation; the second possibility is based on random walk simulation of transport by turbulent diffusion, and is further described in subsection 3.2.

3.1. Distributed parameter model of photosynthesis and photoinhibition in microalgae: Eulerian approach

Accordingly to [1], the transport and reaction phenomena of some species or components describes the following equation (where $c_i = c_i(\vec{r}, t)$ is either a species concentration or cell density):

$$\frac{\partial c_i}{\partial t} + \nabla \cdot (\vec{v} c_i) - \nabla \cdot (D_e \nabla c_i) = R \ , \quad i = 1, ..., m, \tag{10}$$

where R is the reaction (source) term, $\vec{v}$ is the velocity flow field, and $\vec{r}$ stands for a vector of space coordinates. $D_e(\vec{r})$ is the dispersion coefficient (generally the tensor of second order), which corresponds to the diffusion coefficient in microstructure description and becomes mere empirical parameter suitably describing mixing in the system. D_e is influenced by the molecular diffusion and velocity profile (this explains why D_e is spatially dependent). When mixing is mainly caused by the turbulent micro-eddies, the phenomenon is called the turbulent diffusion and a *turbulent diffusion coefficient* is introduced, e.g. in [1].

The initial condition and boundary condition (impermeability of PBR walls, i.e. domain boundary ∂V) to (10) are following:

$$c_{i_0} = c_i(\vec{r}, t_0), \ \nabla c_i(\partial V, t) = 0, \ i = 1, ..., m. \tag{11}$$

The solution of transport equation (10-11) usually causes many complications residing in fact that the relevant transport and reaction phenomena are multi-scale. If we realize that the characteristic time of microalgae growth (e.g. doubling time $t_g := \frac{ln(2)}{\mu}$) is in order of hours, and the the characteristic time of turbulent diffusion ($t_d := \frac{L^2}{D_e}$) is in order of seconds (similarly that of convective transport $t_c := \frac{L}{v}$), then actually only two alternatives exist: (i) to neglect the details concerning mixing phenomena, e.g. by accepting the hypothesis that the entire cell culture dispersed in medium was homogenized at each calculation step (cf. [13], where the time step Δt was set to one hour), and (ii) to observe the changes due to the hydrodynamic mixing and neglect those of biochemical

reaction. Both alternatives completely lose the coupling between transport and reaction phenomena, which qualify the corresponding modelling framework as unsatisfactory.

Our proposition to resolve about mentioned difficulties is based on the extension of PSF model "into space". The stochastic formulation of PSF model, as described in Section 2, is not unique: instead of one photosynthetic factory (with three states), we can imagine as many factories as cells in the cultivation system (i.e. PBR). Each microalgae cell with certain probability stays in its current state or is transformed into one of the remaining states, and at he same time it travels inside the PBR. Assuming we know the irradiance distribution in PBR, i.e. $u = u(\vec{r}, t)$, then we evaluate the specific growth rate not only as the value proportional to the temporal average of the activate state, cf. (6), but also the spatial averaging takes place:

$$\mu = q_2 q_3 (1 + q_5) \frac{1}{t_f - t_0} \int_{t_0}^{t_f} \left(\frac{1}{V} \int_V y_A(\vec{r}, t) \mathrm{d}V \right) \mathrm{d}t \ . \tag{12}$$

The only thing which rests to explain is how to introduce into the transport equation (10) the reaction term coherently with PSF model. Let us evaluate the PSF model states as relative concentrations (molar fractions) of microbial cells in respective state (R, A, or B). Let define the variables c_i as the concentrations of cells in respective states of PSF model, and c as an overall cell concentration. The concentrations are generally varying in time and space $c_i = c_i(x, t),\ i \in \{R, A, B\}$, nevertheless it holds: $c = c_R + c_A + c_B$. Consequently, without loss of precision, we re-define the state vector of PSF model as follows:

$$y = (y_R, y_A, y_B)^\top := \frac{1}{c} \ (c_R, c_A, c_B)^\top . \tag{13}$$

Furthermore, after dividing (10) by c, we can substitute the right hand side of PSF model equation (3) as the reaction term in the right hand side of the following (14):

$$\frac{\partial y}{\partial t} + \nabla \cdot (\vec{v} y) - \nabla \cdot (D_e \nabla y) = \big[\mathcal{A} + u(\vec{r}, t) \mathcal{B} \big] y \ . \tag{14}$$

Equation (14) with the corresponding initial and boundary condition (11) represents the PDE based model for describing multi-scale transport and reaction phenomena in a general PBR. To illustrate the reliability of our approach, we will analyze in Section 4, as a case study, the microalgae growth in a simple rectangular PBR.

3.2. Distributed parameter model of photosynthesis and photoinhibition in microalgae: Lagrangian approach

In our Lagrangian based modelling approach, both the biochemical reaction and transport are treated in a stochastic manner. This brings several advantages over the classical PDE based approach, high potential of parallel implementation, as described further, being one of them. Stochastic model of the transport

is based on a discrete random walk model which reflects the spatially dependent turbulent diffusion coefficient. It is this coefficient that binds the stochastic behavior to the real hydrodynamic conditions in the simulated domain. Spatial dependence of the diffusion coefficient may be obtained by classical means, i.e. CFD (Computational Fluid Dynamics) numerical simulation for the given geometry. With respect to the implementation - mainly computational issues, the apparent advantage of this approach is mutual independence of the individual cells under cultivation, where every cell is represented by an independent photosynthetic factory, whose only input parameter is spatially dependent irradiance $u(\vec{r})$ (the temporal variation of irradiance is neglected, because it occurs in several order slower time-scale). The succession of states of the individual cells (R, A, and B) forms a Markov chain, with $\mathcal{A} + u\mathcal{B}$ being the system matrix of (3), the infinitesimal generator, see e.g. [2] and references within there. The details about algorithm design and implementation are discussed in the following Section 4.

4. Simulation results: Random walk vs. Finite difference method

4.1. Problem formulation

We aim to simulate, eventually to optimize microalgae cell growth in a PBR. For the sake of clarity, we further suppose the rectangular, axi-symmetrical PBR geometry, illuminated from one side, i.e. the irradiance level is decreasing from the PBR wall to PBR core, cf. Fig. 1. Thus, the PBR volume (our computational domain) can be divided into layers with the same irradiance level. Moreover, if the flow field in the PBR is stationary and does not depend on the coordinates perpendicular to the direction of light gradient, then we can neglect the cell motion over the layers with the same irradiance level, transforming the 3D problem into the one-dimensional. It means that only the cell motion in direction of light gradient is of most interest. This motion is caused by the turbulent diffusion (hydrodynamic dispersion) characterized by an only parameter $D_e(r)$, i.e. by the dispersion coefficient (a tensor of second order in 3D case).

As stated before, the only input parameter determining the bio-reaction rate is the spatially dependent irradiance $u(r)$. Here we announce the exponential, so-called Lambert-Beer law, and the relation for average (absorbed) irradiance, in the form:

$$u(r) = u_0 \; e^{-\Lambda r} \;, \;\; u_{av} = u_0 \frac{1 - e^{-\Lambda L}}{\Lambda L} \;, \tag{15}$$

where u_0 is the incident irradiance, Λ is the attenuation coefficient (unit: m^{-1}) and L is the PBR thickness in direction of light gradient. It is convenient to define a dimensionless "thickness constant" $k > 0$ as follows: $L := k \; r_{1/2}$, where $r_{1/2} := \frac{\ln(2)}{\Lambda}$, is the length interval (unit: m) making diminish the intensity of light to one half. Furthermore, we introduce the dimensionless spatial coordinate x and as follows:

$$x := \frac{r}{L} \;, \;\; x \in [0, 1] \;. \tag{16}$$

After this transform, we introduce also the dimensionless dispersion coefficient $p(x)$ by $D_e := p(x)\ D_0$, where D_0 is a constant with some characteristic value, unit: $\mathrm{m^2s^{-1}}$. According to [1], nearly all physical exchange is linearly dependent on the driving force. Hence, for the growing power supply to the PBR pumping device we expect D_0 proportionally grows, meanwhile the D_e shape (i.e. $p(x)$) remains constant. For $p(x)$ we propose the following relation:

$$p(x) := p_0 + p_1 \left[1 - (|2x - 1|)^n\right] \ , \tag{17}$$

where p_0, p_1, n are dimensionless positive constants (to be determined empirically).

All the values needed to perform further calculations are summarized in Table 1:

u_0	D_0	k	L	p_0	p_1	q_2	q_4	n	$y_R(t_0)$	$y_A(t_0)$	$y_B(t_0)$
$\frac{8\ln(2)}{1-2^{-8}}$	0.0001	8	0.02	2	1	0.3	0.5	2	1	0	0

Table 1: Parameters summary

The values representing initial guess for operating conditions (to be optimized) are in the first two columns, the middle seven data are empirical constants, and the last three values are initial conditions for simulation of time course of PSF states. It is important at this stage to point out that the empirical data have an illustrative and testing purpose only.

4.2. Lagrangian simulation

The Lagrangian simulation algorithm was designed with parallel platform implementation in mind and was performed both on the classical PC and a parallel platform - namely CUDA (Compute Unified Device Architecture) architecture. Random walk model was implemented on top of the Mersenne Twister parallel random number generator in combination with Box-Muller transformation. With this parallel reimplementation on CUDA we were able to get an additional 90-fold gain in speed when compared to the single threaded implementation running on PC.

The simulation results for the Lagrangian simulation are summarized in Tables 2 and 3

From the last columns it is evident that the steady state was reached. All the simulation parameters besides D_0 were the same as shown in Table 1. The particular value $D_0 = 0.5$ was found empirically as a minimal D_0 at which the culture growth is not transport-limited, i.e. the mixing is sufficient.

Time [s]	0	1	10	50	100	500	1000	2000	3000	4000	5000
$y_{R_{av}}$	1.00	0.61	0.21	0.20	0.21	0.20	0.20	0.18	0.17	0.17	0.17
$y_{A_{av}}$	0.00	0.39	0.79	0.79	0.78	0.74	0.70	0.66	0.65	0.62	0.62
$y_{B_{av}}$	0.00	0.00	0.00	1.00	0.01	0.06	0.10	0.16	0.18	0.21	0.21

Table 2: Random walk simulation results, $D_0 = 0.5$, maximum growth rate reached

Time [s]	0	50	100	500	1000	2000	3000	4000	5000	10000
$y_{R_{av}}$	1.00	0.43	0.42	0.40	0.38	0.36	0.34	0.33	0.33	0.33
$y_{A_{av}}$	0.00	0.57	0.56	0.54	0.51	0.47	0.46	0.45	0.44	0.44
$y_{B_{av}}$	0.00	0.00	0.02	0.06	0.11	0.17	0.20	0.22	0.23	0.23

Table 3: Random walk simulation results, $D_0 = 0.005$

4.3. Eulerian simulation and optimization of incident irradiance u_0

Based on the previous time dependent Lagrangian simulation results, we argue that all PSF states are approaching some value $y_{i_{ss}}(x) = \lim_{t\to\infty} y_i(x,t),\ i \in \{R, A, B\}$, depending on the external inputs u_0 and D_0 only. Moreover, the inhibited state $y_{B_{ss}}(x)$ is nearly constant across the PBR (data not shown) and holds: $y_B = y_{B\,ss}(u_{av})$.

Consequently, based on the above reasons, we modify the transport-reaction system (14) as follows: first, let us put $\frac{\partial c}{\partial t} = 0$, then employ (9), then we obtain (omitting the upper index "F"):

$$-\left[p(x)y_A'\right]' + q(x)\ y_A = q(x)\ y_{A_\infty},\ \ y_A'(0) = 0,\ y_A'(1) = 0\ , \tag{18}$$

where $q(x) := \frac{q_4(u(x)+q_2)\ L^2}{D_0}$. The function $y_{A_\infty}(x)$ is calculated as the steady state solution of (9):

$$\begin{aligned} y_{A_\infty}(x) &= \frac{u(x)}{u(x)+q_2}\left[1 - y_{B\,ss}(u_{av})\right] \\ &= \frac{u(x)}{u(x)+q_2}\left[\frac{u_{av}+q_2}{q_2({u_{av}}^2 + u_{av}/q_2 + 1)}\right]. \end{aligned} \tag{19}$$

Let the characteristic number, the so-called *Damköhler number* of second type be defined as

$$Da_{II} := \frac{q_4\ L^2}{D_0}, \tag{20}$$

then $q(x) := (u(x)+q_2)\ Da_{II}$ holds. Further, the dependence of the solution of (18) on Da_{II} will be studied.

The boundary value problem with Neumann initial conditions and inhomogeneous right-hand side (18) has a lot of nice properties. It is symmetric and positive and the corresponding linear differential operator of the second order

$$L(y_A) = -\left[p(x)y_A'\right]' + q(x)\ y_A,$$

is self-adjoint. As $q(x) > 0$, problem (18) has a unique solution (see e.g. [20], [24]). It was solved numerically using a following finite difference scheme with uniformly distributed nodes which leads to a symmetric and positive definite system of linear equations for unknown values

$$y_{Ai} = y_A(x_i) \equiv y_A(x_i, \infty), \quad i = 0, \ldots, N,$$

with a tridiagonal matrix:

$$\begin{pmatrix} a_0 & b_0 & 0 & \ldots & 0 \\ b_0 & a_1 & \ddots & \ddots & \vdots \\ 0 & \ddots & \ddots & \ddots & 0 \\ \vdots & \ddots & \ddots & \ddots & b_{N-1} \\ 0 & \ldots & 0 & b_{N-1} & a_N \end{pmatrix} \begin{pmatrix} y_{A0} \\ \vdots \\ \vdots \\ \vdots \\ y_{AN} \end{pmatrix} = \begin{pmatrix} g_0 \\ \vdots \\ \vdots \\ \vdots \\ g_N \end{pmatrix}$$

where

$$\begin{aligned} a_0 &= p(x_0 + h/2) + h^2 q(x_0)/2, \\ a_i &= p(x_i - h/2) + p(x_i + h/2) + h^2 q(x_i), \quad i = 1, \ldots, N-1, \\ a_n &= p(x_N - h/2) + h^2 q(x_N)/2, \\ b_i &= -p(x_i + h/2), \quad i = 0, \ldots, N-1, \\ g_0 &= h^2 f(x_0)/2, \\ g_i &= h^2 f(x_i), \quad i = 1, \ldots, N-1, \\ g_n &= h^2 f(x_N)/2. \end{aligned}$$

Here $f(x) = q(x)\ y_{A_\infty}(x)$, $x_i = ih$, and $h = \frac{1}{N}$, where N denotes the number of nodes. Such a scheme approximates the exact solution of the boundary value problem (18) with accuracy of order h^2.

In our numerical experiments we have chosen the values from Table 1 together with $N = 1000$. The following Fig. 4 shows dependence of the solution on the *Damköhler number* Da_{II}. We can see that the solution approaches a constant value $y_A(x, \infty) = 0.625$ for $Da_{II} \to 0$. Let us see that the solution becomes flatter for decreasing Da_{II} and for $Da_{II} = 0.2$ the solution is nearly constant.

One of the most important issues in biotechnological literature is the analysis of bioreactor performance. In our context, the measure of PBR performance is the photosynthetic productivity which is directly proportional to the specific growth rate, cf. (12). For the PBR continuous operation mode and after certain operations leading to (18), we define the cost functional (performance index) as follows:

$$J = \int_0^1 y_A(x, \infty) \mathrm{d}x, \tag{21}$$

recalling that $y_A(x, \infty)$ is a solution to (18). Further, we can formulate the optimization problem residing in *maximizing* the performance index J, having u_0 and/or Da_{II} as optimization parameters.

The next Fig. 5 shows dependence of J on Da_{II}, for the incident irradiance u_0 taken from Table 1. The maximum value arises for $Da_{II} \to 0$ and its value is $J = 0.625$. Minimum value in (21) arises when the solution of (18) is $y_A(x, \infty) = y_{A_\infty}(x)$, which leads to a value $J \approx 0.4254$.

Remark 2: Notice that the value $J = 0.625$ corresponds to the value $y_{A_{ss}}(1) = \frac{1}{2q_2+1}$, cf. (7). This means that the ODE system (18), for the case $Da_{II} \to 0$, performs the "averaging" of $u(x)$.

We have made several simulations for various u_0 and the values of J were smaller than those for u_0 taken from Table 1. This is a numerical confirmation of the hypothesis often mentioned in biotechnological literature.

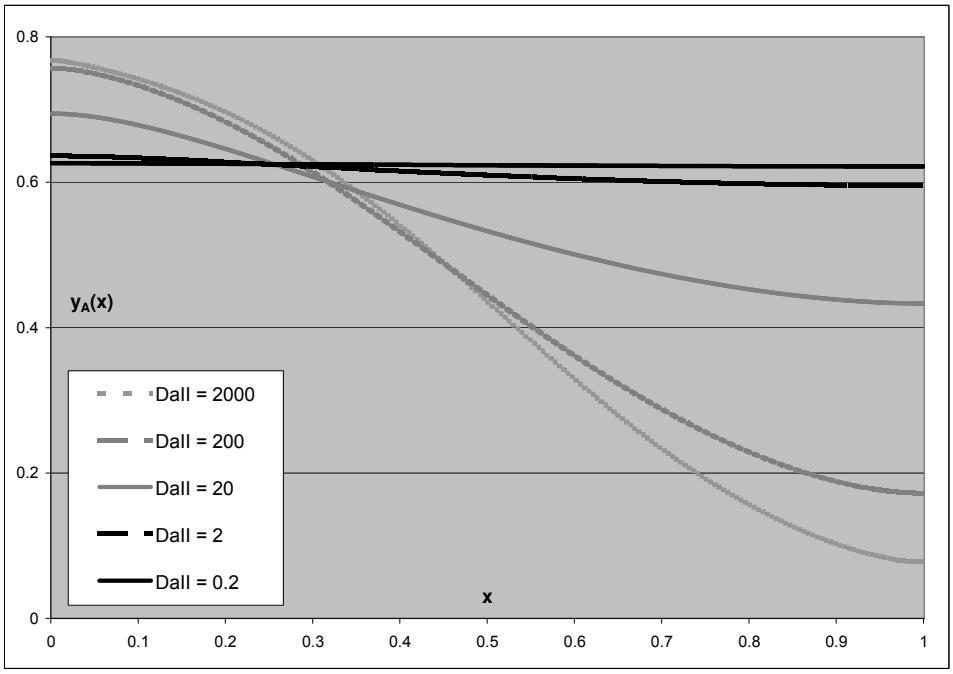

Figure 4: Approximate solution to (18).

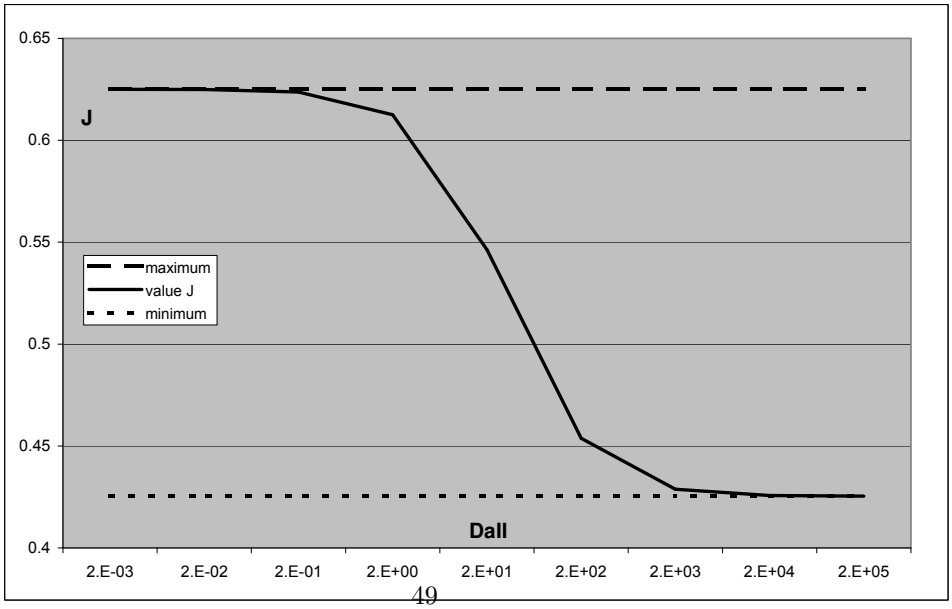

Figure 5: Performance index J vs. Da_{II}.

5. Conclusions

The purpose of this paper was to present an extension of a lumped parameter model of photosynthetic microorganism growth to the domain with heterogeneously distributed relevant parameters, e.g. irradiance and turbulent diffusion (hydrodynamic dispersion). The principal problem was to find how to reconcile the multi-scale problem in such a manner, that the corresponding modelling framework was sensitive to all relevant phenomena. The key decision was to adopt the model of photosynthetic factory (PSF model), which operates in three time-scales, being sensitive to the time-scale of turbulent diffusion.

Both approaches and corresponding numerical techniques, i.e. random walk and finite difference method, show the consistent results, proving the viability of our efforts. The advantage of the stationary PDE based model resides in less computationally expensive solution of optimization of PBR operating conditions. On the other hand, Lagrangian approach and random walk technique permit the parallel stochastic simulation of microalgal growth in a real time.

References

[1] W.J. Beek, K.M.K. Muttzall, J.W. van Heuven, Transport Phenomena, Wiley & Sons, 2000.

[2] E. Bohl, I. Marek, Input-output systems in biology and chemistry and a class of mathematical models describing them, Applications of Mathematics, 50 (2005) 219–245.

[3] S. Čelikovský, On the continuous dependence of trajectories of bilinear systems on controls and its applications, Kybernetika, 24 (1988) 278–292.

[4] S. Čelikovský, Š. Papáček, A. Cervantes-Herrera, J. Ruiz-León, Singular Perturbation Based Solution to Optimal Microalgal Growth Problem and its Infinite Time Horizon Analysis, TAC IEEE, 55(3) (2010) 767–772.

[5] I.J. Dunn, E. Heinzle, J. Ingham, J.E. Přenosil, Biological Reaction Engineering, VCH, Weinheim - New York - Basel - Cambridge, 1992.

[6] P.H.C. Eilers, J.C.H. Peeters, A model for the relationship between light intensity and the rate of photosynthesis in phytoplankton, Ecological Modelling, 42 (1988) 199–215.

[7] P.H.C. Eilers, J.C.H. Peeters, Dynamic behaviour of a model for photosynthesis and photoinhibition, Ecological Modelling, 69 (1993) 113–133.

[8] M. Janssen, J. Tramper, L.R. Mur, R.H. Wijffels, Enclosed Outdoor Photobioreactors: Light Regime, Photosynthetic Efficiency, Scale-Up, and Future Prospects, Biotechnology and Bioengineering, 81 (2003) 193–210.

[9] T. Kmeť, M. Straškraba, P. Mauersberger, A mechanistic model of the adaptation of phytoplankton photosynthesis. Bulletin of Mathematical Biology, 55 (1993) 259–275.

[10] H.P. Luo, A. Kemoun, M.H. Al-Dahhan, J.M. Fernández Sevilla, J.L. García Sánchez, F. García Camacho, E. Molina Grima, Analysis of photobioreactors for culturing high-value microalgae and cyanobacteria via an advanced diagnostic technique: CARPT., Chemical Engineering Science, 58(12) (2003) 2519-2527.

[11] J. Masojídek, Š. Papáček, V. Jirka, J. Červený, J. Kunc, J. Korečko, M. Sergejevová, O. Verbovikova, J. Kopecký, D. Štys, G. Torzillo, A Closed Solar Photobioreactor for Cultivation of Microalgae under Supra-High Irradiances: Basic Design and Performance of Pilot Plant. J. Appl. Phycol., 15 (2003) 239–248.

[12] E. Molina, F.G. Acien, F. Garcia, F. Camacho, Y. Chisti, Scale-up of tubular photobioreactors, J. of Biotechnology, 92 (2000) 113–131.

[13] A. Muller-Feuga, R. Le Guédes, J. Pruvost, Benefits and limitations of modeling for optimization of *Porphyridium cruentum* cultures in an annular photobioreactor, J. of Biotechnology, 103 (2003) 153–163.

[14] L. Nedbal, V. Tichý, F. Xiong, J.U. Grobbelaar, Microscopic green algae and cyanobacteria in high-frequency intermittent light, J. Appl. Phycol., 8 (1996) 325–333.

[15] Š. Papáček, S. Čelikovský, D. Štys, J. Ruiz-León, Bilinear System as Modelling Framework for Analysis of Microalgal Growth, Kybernetika, 43 (2007) 1–20.

[16] Š. Papáček, S. Čelikovský, J. Ruiz-León, Optimal Feedback Control of Microalgal Growth Based on the Slow Reduction, in: Proc. IFAC World Congress 2008, Seoul, Korea, July 2008, pp. 14588–14593.

[17] Š. Papáček, S. Čelikovský, B. Rehák, D. Štys, Experimental design for parameter estimation of two time-scale model of photosynthesis and photoinhibition in microalgae, Math. Comput. Simul., 80 (2010) 1302–1309.

[18] J. Pruvost, J. Legrand, P. Legentilhomme, A. Muller-Feuga, Lagrangian trajectory model for turbulent swirling flow in an annular cell: comparison with residence time distribution measurements, Chemical Engineering Science, 57 (2002) 205–1215.

[19] B. Rehák, S. Čelikovský, Š. Papáček, Model for Photosynthesis and Photoinhibition: Parameter Identification Based on the Harmonic Irradiation O_2 Response Measurement, Joint Special Issue of TAC IEEE and TCAS IEEE, (2008) 101–108.

[20] K. Rektorys, Přehled užité matematiky, Nakladatelství Prometheus, Praha, 1995.

[21] K. Schugerl, K.H. Bellgardt (Eds), Bioreaction Engineering, Modeling and Control, Springer-Verlag, Berlin, Heidelberg, 2000.

[22] K.L. Terry, Photosynthesis in Modulated Light: Quantitative Dependence of Photosynthetic Enhancement on Flashing Rate, Biotechnology and Bioengineering, 28 (1986) 988-995.

[23] A.N. Tichonov, A.B. Vasileva, A.G. Sveshnikov, Differential Equations, Nauka, Moscow, 1980 (in Russian).

[24] E. Vitásek, Numerické metody, Nakladatelství technické literatury, Praha, 1987.

[25] X. Wu, J.C. Merchuk, A model integrating fluid dynamics in photosynthesis and photoinhibition processes, Chemical Engineering Science, 56 (2001) 3527-3538.

2.3 Paper III - Lattice Boltzmann method in bioreactor design and simulation

In this paper a Lattice Boltzmann method (LBM) based approach to the simulation of the transport phenomena is presented and validated on the case of the Couette-Taylor photobioreactor (CTBR). This photobioreactor presents a challenge from the boundary conditions perspective because of the circular rotating wall that provides mixing in the device. The correct treatment of this boundary condition in LBM is identified and the validity of the LBM solver was proven by the successful comparison of the analytical solutions of the Couette cylindrical flow and the simulated results.

Further the performance potential of both the LBM method for the transport phenomena and the method of the Photosynthetic Factory (PSF) for the reaction phenomena were studied and the resulting performance enhancement based on the grid size and cell count is presented.

Lattice Boltzmann method in bioreactor design and simulation

Václav Štumbauer[a], Karel Petera[b], Dalibor Štys[a]

[a] *Institute of Physical Biology, University of South Bohemia, 373 33 Nové Hrady, Czech Republic*
[b] *Faculty of Mechanical Engineering, Czech Technical University in Prague, Technicka 4, 166 07 Prague 6, Czech Republic*

Abstract

The Lattice Boltzmann Method (LBM) for fluid flow has already proven itself a viable alternative to classical CFD (Computational Fluid Dynamics) methods based on discrete scheme application to Navier Stokes equations governing the fluid flow. In this paper, we aim to verify the applicability of LBM in a special case of a Couette-Taylor Photobioreactor – a device comprised of two coaxial cylinders with a rotating inner wall. An appropriate numerical approach to the curved moving wall boundary condition is presented and verified by velocity flow field comparison with analytical solution. The parallelism potential of LBM is exploited on the parallel platform of CUDA (Compute Unified Device Architecture). Microalgae growth in the flow field simulated by LBM is based on the Model of Photosynthetic Factory (PSF) treated in a parallel stochastic manner and implemented also on the parallel platform of CUDA. Parallel stochastic PSF solver has been validated by comparison with analytical solution of PSF model at constant irradiance.

Keywords: Lattice Boltzmann Method, bioreactor simulation, photosynthetic factory
PACS: 93C10, 37N25

1. Introduction

Microalgae has gained a lot of attention due to its wide area of applicability. It has been shown that it has a high potential as a source of renewable energy – i.e. biofuels [1, 2] and as a source of wide spectra of valuable bioactive compounds. It may also be used in other environmental applications like CO_2 sequestration, bioremediation [3], waste water treatment and others.

Email addresses: stumbav@gmail.com (Václav Štumbauer), karel.petera@fs.cvut.cz (Karel Petera), stys@jcu.cz (Dalibor Štys)

Microalgae is nowadays cultivated mostly in either large open systems or closed photobioreactors [4]. While the outdoor open systems present a lower construction and operating costs they have several disadvantages over the closed systems – e.g. higher risk of contamination (i.e. they're not suitable for all the strains) and higher harvesting costs due to lower biomass concentration [4]. Within the scope of our work we focus on a special case of a closed system – the so-called Couette-Taylor photobioreactor [5].

Mainly due to the complex multi-scale processes governing the microalgae growth in multi-phase, multi-component flow the microalgae cultivation still is rather an empirical process [4]. Bezzo et al. [6] have used a hybrid multizonal/CFD approach to tackle the problem. Papáček et al. have studied a multi-scale lumped parameter model for description of principal physiological processes in microalgae [7, 8, 9, 10] and have successfully employed the hybrid multizonal/CFD method in the case of Couette-Taylor photobioreactor [5] with inter-compartment flows estimated by means of classical CFD. In our previous work [11, 12] we have introduced an alternative approach based on random walk with spatially dependent dispersion coefficient devised from a CFD simulation.

With the work presented we would like to contribute to a more deterministic bioreactor design with a method based on parallel LBM fluid flow simulation and parallel stochastic implementation of PSF.

2. Materials and Methods

2.1. Couette-Taylor Photobioreactor

Couette-Taylor photobioreactor (CTBR) is a tubular device comprised of two coaxial cylinders. Rotation of the inner cylinder provides suspension mixing, which is important for mass transfer of nutrients and waste-products and for intermittent illumination of cultivated microalgae. Both the bioreactor walls are translucent and a constant outer wall irradiance is supposed. This yields an irradiance profile in the following form:

$$u(r) = \frac{U_0 R_o}{r}(\exp^{-\Lambda(R_o - r)} + \exp^{-\Lambda(R_o + r)}) \tag{1}$$

where U_0 is light intensity at the outer wall, R_o radius of the outer wall and Λ is a microalgae concentration dependent light attenuation coefficient.

All dense microalgae cultures require CO_2 supply, our CTBR is supplied with CO_2 by bubbling the inner volume with compressed air with 5% CO_2. Another important advantage of the device is the possibility to explore wide range of "well-defined"shear stress and its impact on microalgae growth. One of the reasons for choosing this specific device is the long-term goal of enhancing the microalgae growth models with mechanical stress tensor dependence.

2.2. Lattice Boltzmann method

The lattice Boltzmann method [13] has gained a lot of attention in diverse areas because of its ability to simulate complex flows, straight-forward imple-

mentation and parallelism potential. Instead of solving the Navier-Stokes equations governing the fluid flow, it simulates the flow by particles that are streamed and collided over a discrete lattice. LBM can be regarded as a solution to the Boltzmann single particle distribution function in discrete time and space.

Various discrete schemes and relaxation models towards the local equilibrium exist. A scheme with nineteen discrete directions (D3Q19) is widely adopted in literature for three dimensional flow simulation as a trade-off between computational costs, accuracy and stability. D3Q19 scheme together with the so-called BGK [14] single-time-relaxation model to local equilibrium has been employed in our approach. The following equation expresses both the streaming and collision step:

$$f_a(\mathbf{x} + \mathbf{e}_a \Delta t, t + \Delta t) = f_a(\mathbf{x}, t) - \frac{[f_a(\mathbf{x}, t) - f_a^{eq}(\mathbf{x}, t)]}{\tau} \tag{2}$$

Where f_a stands for a density distribution function along direction a, $\mathbf{e}_a$ is a particle velocity vector in the direction a, Δt is a time step and τ is the 'single-relaxation-time'(SRT) which is related to kinematic viscosity in the following form:$\nu = \frac{1}{3}(\tau - \frac{1}{2})$.

Equilibrium density $f_a^{eq}(\mathbf{x}, t)$ is in BGK SRT model calculated as follows:

$$f_a^{eq}(\mathbf{x}, t) = w_a \rho(\mathbf{x}, t) \left[1 + \frac{\mathbf{e}_a \cdot \mathbf{u}(\mathbf{x}, \mathbf{t})}{c_s^2} + \frac{(\mathbf{e}_a \cdot \mathbf{u}(\mathbf{x}, t))^2}{2c_s^4} - \frac{\mathbf{u}^2(\mathbf{x}, t)}{2c_s^2} \right] \tag{3}$$

where $\mathbf{u}(\mathbf{x}, t)$ stands for macroscopic velocity, ρ for the macroscopic density, c_s for lattice speed of sound $c_s = \frac{1}{\sqrt{3}}$ and w_a for weighting coefficients:

$$w_a = \begin{cases} \frac{2}{36} & 1 \leq a \leq 6 \\ \frac{1}{36} & 7 \leq a \leq 18 \\ \frac{12}{36} & a = 19 \end{cases} \tag{4}$$

The required macroscopic variables may be recovered from the density distribution function in the following way:

$$\rho(\mathbf{x}, t) = \sum_a f_a \tag{5}$$

$$\mathbf{u}(\mathbf{x}, t) = \frac{1}{\rho(\mathbf{x}, t)} \sum_a f_a \mathbf{e_a} \tag{6}$$

2.2.1. Curved velocity boundary treatment

Interaction with the solid wall in LBM is mostly solved by bounce-back boundary condition. Second order accuracy is in the case of the bounce-back condition achieved when the boundary is placed in the middle between the fluid and outer lattice node – the so called half-way bounce-back [15]. Zou and He also proposed a straight wall velocity boundary treatment based on the idea of bounce-back of non-equilibrium parts of the distribution function [15]. As for

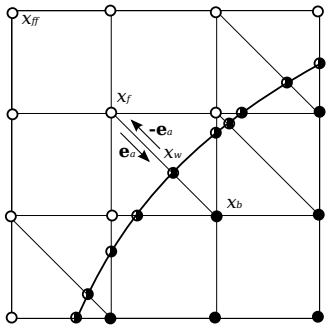

Figure 1: Curved boundary depicted against a regular lattice.

the case of a curved boundary, the boundary often lies somewhere in-between the fluid and outer node and a special treatment is required to preserve the accuracy.

Most of the curved boundary treatments are based on interpolation of the unknown densities based on known information from the surroundings of the boundary node – see e.g. [16, 17, 18, 19]. In this study we've employed a model of Filippova and Hänel [16] which was further enhanced for better stability by Mei et al. [18].

Figure 1 depicts the scenario of a curved boundary, where empty circles stand for fluid nodes, full circles for the outside nodes and half-filled circles for the intersections of the wall with the lattice links. The interpolation takes into account the distance between the boundary and the fluid node in the form of the following ratio Δ:

$$\Delta = \frac{|\mathbf{x}_f - \mathbf{x}_w|}{|\mathbf{x}_f - \mathbf{x}_b|} \tag{7}$$

Based on the value of Δ, an imaginary velocity for interpolation $\mathbf{u}_{bf}$ and a weighting factor χ are calculated:

$$\mathbf{u}_{bf} = \mathbf{u_{ff}} = \mathbf{u}(\mathbf{x}_{ff}, t), \chi = \frac{2\Delta - 1}{\tau - 2}, \text{ if } 0 \leq \Delta < \frac{1}{2} \tag{8}$$

$$\mathbf{u}_{bf} = (1 - \frac{3}{2\Delta})\mathbf{u}_f + \frac{3}{2\Delta}\mathbf{u}_w, \chi = \frac{2\Delta - 1}{\tau + \frac{1}{2}}, \text{ if } \frac{1}{2} \leq \Delta < 1 \tag{9}$$

Unknown post-collision density $\tilde{f}_{\bar{\alpha}}$ is then calculated as follows:

$$\begin{aligned} \tilde{f}_{\bar{\alpha}}(\mathbf{x_b}, t) = \quad & \tilde{f}_\alpha(\mathbf{x}_f, t) - \chi[\tilde{f}_\alpha(\mathbf{x}_f, t) - f_\alpha^{(eq)}(\mathbf{x}_f, t)] + \\ & + \omega_\alpha \rho(\mathbf{x}_f, t) \tfrac{3}{c^2} \mathbf{e}_\alpha \cdot [\chi(\mathbf{u}_{bf} - \mathbf{u}_f) - 2\mathbf{u}_w] \end{aligned} \tag{10}$$

2.2.2. Parallelization

Parallelization of LBM is rather straight-forward. All the microscopic densities have a memory block of their own. During the streaming step and interpolated boundary evaluation, these blocks are copied into arrays and mapped as 3D textures for memory access optimization. Texture based streaming also simplify the implementation of periodic boundary conditions.

2.3. Photosynthetic factory

The so-called Photosynthetic Factory model [20, 21] has been employed for microalgae growth simulation in the 3D flow field of homogeneously irradiated CTBR. Irradiance is the sole input parameter of the model and the model exhibits the important property of 'integrating' fast irradiance changes. Thus in dense well-mixed cultures all microalgae cells may be exposed to irradiance intermittently and grow as if exposed to an averaged irradiance value. The model is comprised of 3 ODEs and a normalizing condition:

$$1 = x_A + x_I + x_R \tag{11}$$

$$\frac{dx_R}{dt} = \gamma x_A + \delta x_I - \alpha u x_R \tag{12}$$

$$\frac{dx_A}{dt} = -\gamma x_A + \alpha u x_R - \beta u x_A \tag{13}$$

$$\frac{dx_I}{dt} = -\delta x_I + \beta u x_A \tag{14}$$

where x_R, x_A and x_I stand for **resting**, **activated** and **inhibited** microalgae photo states respectively and u stands for the local irradiance intensity. α,β,γ and δ describe the behavior of a particular strain under cultivation.

The actual growth rate is proportional to the averaged amount of activated state:

$$\mu = \kappa\gamma\overline{x_A} - M_e \tag{15}$$

Here M_e stands for metabolism overhead and κ is a constant of proportionality between the growth rate and averaged activated state amount for a particular strain.

2.4. Parallel stochastic treatment

The PSF model has been treated in a stochastic manner. Each microalgae cell is always in one of the possible photo states, no partial state probabilities are stored. Photo states are reevaluated at each time step based on switching probabilities devised from local irradiance intensity and model coefficients α, β, γ and δ. Independence of different microalgae cells makes it an easy task to implement the PSF simulation on the parallel architecture of CUDA.

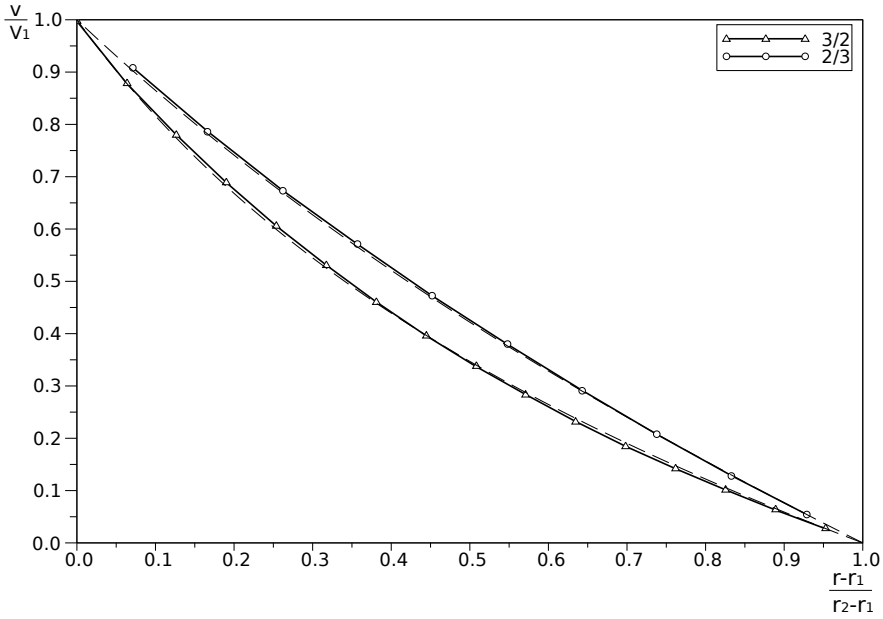

Figure 2: Comparison of simulated cylindrical Couette flow velocity profile with analytical solution at different $\frac{r_1}{r_2-r_1}$.

3. Results

3.1. LBM solver

As a means of validation for the LBM solver in the case of CTBR a cylindrical Couette flow was simulated at various $\frac{r_1}{r_2-r_1}$ and compared with the analytical velocity profile – see figure 2. Analytical solution for the cylindrical Couette flow is as follows:

$$u(r) = Ar + \frac{B}{r}, A = \frac{-\omega_1\nu^2}{1-\nu^2}, B = \frac{\omega_1 r_1^2}{1-\nu^2}, \nu = \frac{r_1}{r_2} \tag{16}$$

Results obtained correspond to the Reynolds number $Re = 6.4$. Computations have been done on a grid of 64×64 nodes in the transverse plane (i.e. the plane perpendicular to CTBR axis).

3.1.1. Speedup

Speedup of LBM solver between CPU implementation and parallel GPU (Graphics Processing Unit) implementation has been measured at various grid sizes and is shown in figure 3. Smaller grid sizes ($16 \times 16 \times 16$) show much lower speedup mainly due to the frequent kernel invocations.

Computations have been done on AMD Athlon^{TM}64 X2 Dual Core Processor 5000+ and GeForce 9800 GT with 512 MB of memory.

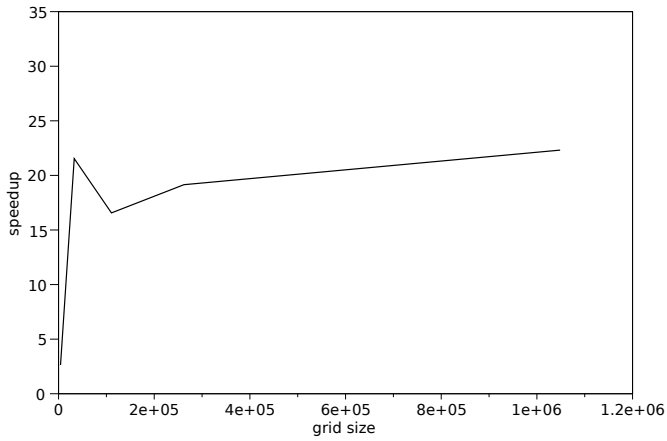

Figure 3: Speedup for the LBM solver implemented both on host CPU and GPU

3.2. PSF solver

To validate the PSF solver a comparison of simulated results with the analytical solution for x_A of the PSF model at constant irradiance has been performed. Figure 4 depicts comparison of averaged simulated results for 8192 microalgae cells and analytical solution at various levels of constant irradiance normalized by the optimal irradiance I_{opt}. Comparison is based on results from [20], where the coefficients have the following relations: $\alpha = 5\beta$, $\gamma = 5\delta$.

3.2.1. Speedup

Speedup obtained in the case of the parallel stochastic implementation of PSF at various cell counts is shown in figure 5. The results are slightly distorted by different random number generator implementations – while on host a Boost library's Mersenne Twister has been used, CUDA platform's cuRand library has been used on GPU. Speedup increased clearly till 8192 cells, then with increasing number of cells it remained almost constant.

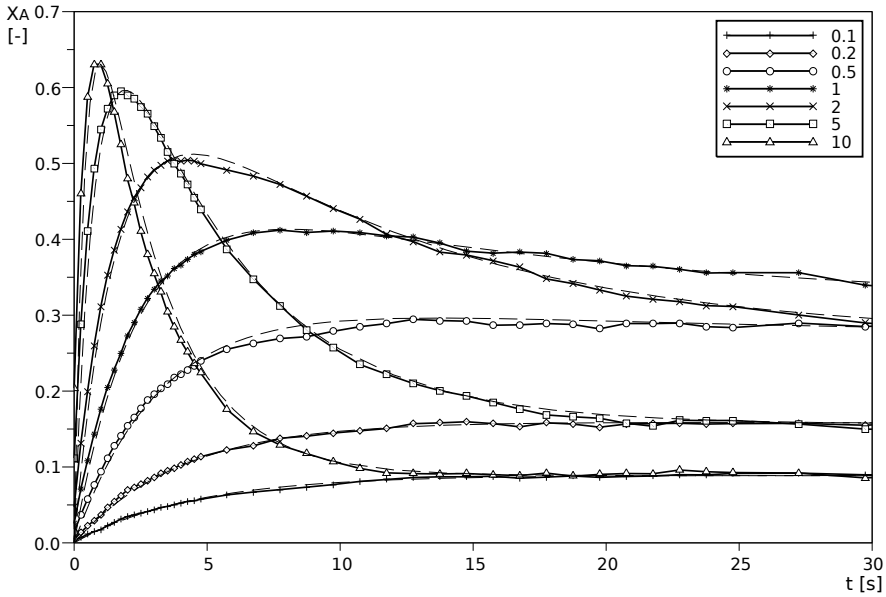

Figure 4: Comparison of simulated PSF results and analytical solution. The activated photosynthetic state x_A (see Eq. 13) is displayed here for different values of constant relative irradiance I/I_{opt}. The dashed lines signify the analytical solution at the respective irradiance levels.

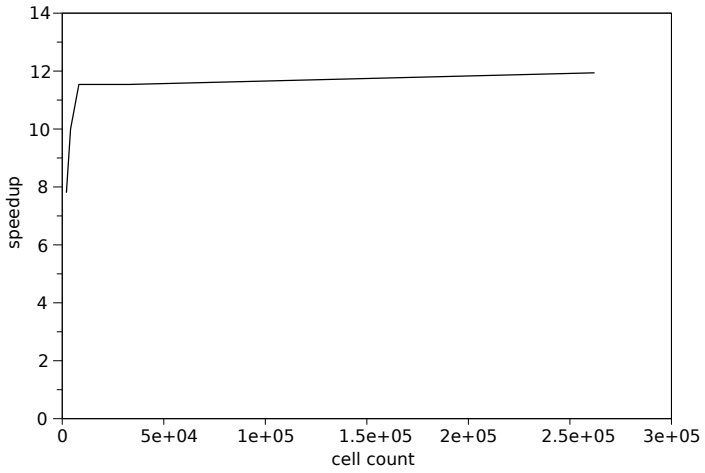

Figure 5: Speedup for the stochastic PSF solver implemented both on host CPU and GPU

4. Conclusions

Within the presented work an alternative approach to bioreactor design and simulation based on parallel implementation of Lattice Boltzmann method for fluid flow and parallel stochastic implementation of Photosynthetic Factory for microalgae growth has been presented. Simulation approach has been validated in the case of cylindrical closed photobioreactor – the so-called Couette-Taylor photobioreactor. Fluid flow has been validated against analytical velocity profiles in the case of cylindrical Couette flow. Parallel stochastic approach to the model of Photosynthetic Factory has been successfully validated by comparison of simulated results and analytical results at constant irradiance.

Acknowledgement

This work was supported by the project "Jihočeské výzkumné centrum akvakultury a biodiverzity hydrocenóz"(CENAKVA), OP VaVpI.

References

[1] Chisti Y.: Biodiesel from microalgae. *Biotechnology Advances*, 25 (2007), 294–306

[2] Schenk P.M. et al.: Second Generation Biofuels: High-Efficiency Microalgae for Biodiesel Production. *Bioenergy Research*, 1 (1), 20–43

[3] Meagher R.B.: Phytoremediation of toxic elemental and organic pollutants. *Current Opinion in Plant Biology*, 3 (2), 153–162

[4] Richmond A.: Handbook of Microalgal Culture: biotechnology and applied phycology. John Wiley and Sons, 2004

[5] Papáček Š., Štys D., Dolínek P., Petera K.: Multicompartment/CFD modelling of transport and reaction processes in Couette-Taylor photobioreactor. *Applied and Computational Mechanics*, 1 (2007), 577–586

[6] Bezzo F., Macchietto S., Pantelides C.C.: Computational issues in hybrid multizonal/computational fluid dynamics models *AIChE Journal*, 51 (2005), 1169–1177

[7] Papáček Š., Čelikovský S., Štys D., Ruiz-León J. : Bilinear System as Modelling Framework for Analysis of Microalgal Growth. *Kybernetika*, vol. 43 (2007), 1–20.

[8] Papáček Š., Čelikovský S., Rehák B., Štys D.: Experimental design for parameter estimation of two time-scale model of photosynthesis and photoinhibition in microalgae. *Mathematics and Computers in Simulation*, 80 (2010), 1302–1309

[9] Rehák, B., Čelikovský S., Papáček, Š.: Model for Photosynthesis and Photoinhibition: Parameter Identification Based on the Harmonic Irradiation O_2 Response Measurement. Joint Special Issue of *TAC IEEE* and *TCAS IEEE*, (2008), 101–108

[10] Čelikovský S., Papáček, Š., Cervantes-Herrera A., Ruiz-León J.: Singular perturbation based solution to optimal microalgal growth and its infinite time horizon analysis. *TAC IEEE*, 55 (3) (2010), 767–772

[11] Papáček Š., Matonoha C., Štumbauer V., Štys D.: Modelling and simulation of photosynthetic microorganism growth: random walk vs. finite difference method. *Mathematics and Computers in Simulation*, in press

[12] Papáček Š., Štumbauer V., Štys D., Petera K., Matonoha C.: Growth impact of hydrodynamic dispersion in a Couette-Taylor bioreactor. *Mathematical and Computer Modelling*, 7–8 (54) (2011), 1791–1795

[13] Succi S.: The Lattice Boltzmann Equation for Fluid Dynamics and Beyond. Oxford University Press, 2001

[14] Bhatnagar P.L., Gross E.P., Krook M.: A model for collision processes in gases. *Physical Review*, 94 (1954), 511–525

[15] Zou Q., He X.: On pressure and velocity boundary conditions for the lattice Boltzmann BGK model. *Physics of Fluids*, 6 (9), 1591–1598

[16] Filippova O., Hänel D.: Grid Refinement for Lattice-BGK Models. *Journal of Computational Physics*, 147 (1998), 219–228

[17] Bouzidi M., Firdaouss M., Lallemand P.: Momentum transfer of a Boltzmann-lattice fluid with boundaries. *Physics of Fluids*, 13 (11), 3452–3459

[18] Mei R., Shyy W., Luo L.S.: Lattice Boltzmann method for 3D flows with curved boundary. *Journal of Computational Physics*, 161 (2000), 680–699

[19] Yu D., Mei R., Shyy W.: A unified boundary treatment in lattice Boltzmann method. New York: AIAA 2003-0953

[20] Eilers, P.H.C., Peeters, J.C.H.: Dynamic behaviour of a model for photosynthesis and photoinhibition. *Ecological Modelling*, 69 (1993), 113–133.

[21] Wu X., Merchuk J.C.: A model integrating fluid dynamics in photosynthesis and photoinhibition processes. *Chemical Engineering Science*, 56 (2001), 3527–3538.

2.4 Paper IV - Modeling and optimization of microalgae growth in photobioreactors: a multidisciplinary multiscale problem

In this paper a formalized unified general PBR modeling approach, consisting of a state and a fluid model, is presented. This model allows the production prediction and operating conditions and control optimization for the general PBR, regardless of the device and cultivated strain. Optimization is based on the following objective function, averaging the productivity over the total cultivation time T and spatial domain Ω:

$$J(d,g) = \frac{1}{meas(\Omega)T} \int_0^T \int_\Omega \mu(x,t) c_x dx dt \tag{2.2}$$

where d and g stand for the design and control variables respectively, μ corresponds to the specific growth rate and c_x to the product concentration.

As a use case of the method, production optimization is presented for the case of the Couette-Taylor photobioreactor.

Modeling and optimization of microalgae growth in photobioreactors: a multidisciplinary multiscale problem

Štěpán Papáček[a], Jiří Jablonský[a], Václav Štumbauer[a], Karel Petera[b], Branislav Rehák[c], Ctirad Matonoha[d]

[a] *University of South Bohemia in Ceske Budejovice, Faculty of Fisheries and Protection of Waters, South Bohemian Research Center of Aquaculture and Biodiversity of Hydrocenoses, Institute of Complex Systems, Zámek 136, 373 33 Nové Hrady, Czech Republic*
spapacek@frov.jcu.cz
[b] *Czech Technical University in Prague, Faculty of Mechanical Engineering, Technicka 4, 166 07 Prague 6, Czech Republic*
[c] *Institute of Information Theory and Automation, Academy of Sciences of the Czech Republic, 182 09 Prague, Czech Republic*
[d] *Institute of Computer Science, Academy of Sciences of the Czech Republic, Pod Vodarenskou vezi 2, 182 07 Prague 8, Czech Republic*

Abstract

Microalgae have potential to be a major biofuel source of the future. To understand biological processes within microalgae and optimize the biofuel production, computational biology plays a key role. Here, we present a multi-timescale modeling approach of microalgae growth in photobioreactors - closed production systems. We propose a multidisciplinary modeling framework to bridge biology (cell growth), physics (hydrodynamics and light distribution) and optimization together. This framework consists of (i) the state system (mass balance equations, e.g., in form of advection-diffusion-reaction PDEs), (ii) the fluid flow equations (e.g., Navier-Stokes equations), and (iii) the optimization problem formulation. To demonstrate this method, the modeling and optimization of microalgae growth in the Couette-Taylor reactor is presented. Moreover, we show the impact of hydrodynamically induced light fluctuation on performance index, i.e. we demonstrate how the flashing light effect can be an intrinsic part of the model. Finally, we discuss further methodological integration with metabolomic-transcriptomic kinetic model which explains cellular concentrations of key metabolites in connection with cell growth.

Keywords: Microalgae, photobioreactor, optimization, multiscale modeling, flashing light effect

Chapter 3

Discussion

The far fetched motivation for this work is a bioreactor CAD (Computer Aided Design) software that would make the production prediction of a general PBR possible. A tool that would also be able to determine the optimal device parameters, such as dimensions with respect to the chosen geometry and operating conditions such as the intensity of mixing, optimal illumination regime/intensity etc. The main reason for which there is still no such a design tool is the multi-disciplinary character and complexity of the relevant phenomena and also the size of the simulated physical domain in the case of the production-scale systems. As it is common in the modelling world, the complexity and the scale of the simulated phenomena may be reduced, but as the example of the unreliable bioreactor scale-up demonstrates quite clearly, not all the problems may be approached in this way. This led to the development of alternative techniques to the bioreactor simulation and their performance optimization on the modern parallel computing platform of Compute Unified Device Architecture (CUDA) - as covered by this work.

The work presents novel approaches to the transport and reaction modelling in photobioreactors (PBR). These are a stochastic Lagrangian transport modelling approach based on the random walk (RW), Lattice-Boltzmann method (LBM) based transport modelling and stochastic simulation of the reaction based on the model of the Photosynthetic Factory (PSF). All of the mentioned approaches have also been implemented on the parallel architecture of CUDA in order to evaluate the potential performance of the method on the modern computing architectures.

The outcomes of the work are general, independent of a particular bioreactor

type in question, nevertheless in order to demonstrate and verify the newly proposed simulation methods two use cases were chosen in the presented papers - the Couette-Taylor photobioreactor (CTBR) and a flat panel photobioreactor.

The first presented paper - *Growth impact of hydrodynamic dispersion in Couette-Taylor bioreactor* - investigates the relation of the microorganism growth with the hydrodynamic dispersion. The research covered by this paper serves as a precursor to the subsequent research of the random walk based method, where the spatially dependent dispersion coefficient serves as a coupling factor between the hydrodynamic conditions inside the bioreactor and the random walk based simulation of the microorganism trajectories. Paper also presents a distributed parameter model extension of the lumped parameter model of the Photosynthetic Factory (PSF) - i.e. the chosen model for the reaction, with distributed parameters being the spatially dependent hydrodynamic dispersion and strongly spatially dependent light intensity. Important contribution of the paper is also the numerical proof of a limiting value of the microorganism growth in the CTBR in dependence on the inner angular velocity and the dependence of the limiting value on the average irradiance.

In the second paper - *Modelling and simulation of photosynthetic microorganism growth: Random walk vs. Finite difference method* - a random walk based bioreactor modelling approach is developed. As it has been already stated, this Lagrangian approach is based on the spatially dependent hydrodynamic dispersion, which may be obtained by the means of the classical CFD methods/available CFD simulation packages. The random walk based method is found to be a usable alternative approach, mainly due to the simulation results corresponding to the Finite Difference Method simulation results on the particular case of the flat panel photobioreactor. Moreover, the function of spatially dependent hydrodynamic dispersion for the case of CTBR is developed and presented.

The third presented paper - *Lattice Boltzmann method in bioreactor design and simulation* - investigates the alternative bioreactor modelling framework based on the Lattice Boltzmann method for solving the transport. In the scope of the paper, a three dimensional parallel Lattice Boltzmann solver is implemented and is coupled with the implementation of the parallel stochastic model of PSF. Both of the presented models are validated against analytic solutions of the relevant phenomenon. The transport solver was validated against analytical solutions of the Couette radial velocity profile corresponding to a lower Taylor number flow in the CTBR. The parallel stochastic PSF solver was validated against the analytical solution for the active photosynthetic state at various ratios of constant light intensity against the optimal light intensity. The paper also further investigates the potential of improving the computational performance

of the presented methods on the parallel architecture of CUDA and gives the performance enhancement ratios for both the transport and reaction at various lattice sizes and cultivated cell count respectively. The paper demonstrates that the Lattice Boltzmann based approach is a viable one and also demonstrates the strength of this approach, which is the considerable potential of the method on the parallel architectures, where by decreasing the computational time, the faster design process is allowed.

The fourth presented paper - *Modeling and optimization of microalgae growth in photobioreactors: a multidisciplinary multiscale problem* - presents a unified modelling approach to the general PBR. Aim of the paper is to have a general modelling framework in which to operate. The proposed framework treats correctly both the transport and the reaction phenomena and, what is important, also couples them correctly together. The approach allows for production prediction and operating conditions and control parameters optimization with respect to the productivity, regardless of the PBR scale or strain under cultivation. As a showcase the proposed state and hydrodynamic model is shown to provide an adequate description of microalgae growth in the Couette-Taylor reactor under hydrodynamically induced high frequency light-dark cycles regime, for which an optimal control problem solution is presented.

Chapter 4

Conclusion

The purpose of the work was to advance the microalgae photobioreactor (PBR) design and modeling. I have addressed two crucial issues. The first issue is the oversimplification of the current models with respect to the modeling of either the transport or of the reaction. Part of this issue is also the incorrect coupling of the transport and reaction processes in the current models. The second issue is computational - it is currently impossible to perform the simulation of a general PBR in a time that would allow a viable optimization of the device parameters and operating conditions. This issue may be approached by either searching for different (computationally more suitable) models or by increasing the performance of the available models as demonstrated below.

My results addressing the aforementioned issues are the following:

- **Unified general framework for PBR modeling**

  I have developed a new Lagrangian PBR model that treats correctly both the transport and reaction processes in a general PBR and couples these processes correctly together. The model itself is independent on the PBR geometry and the used reaction model. With respect to the model implementation, the reaction model of the Photosynthetic Factory (PSF) has been identified as an optimal compromise between the sophisticated physiological models and the simple and insufficient steady-state reaction models. For the first time, the Lattice-Boltzmann method (LBM) for fluid flow simulation has been demonstrated as a suitable and advantageous alternative to the classical Computational Fluid Dynamics (CFD) methods

in solving the transport processes in a PBR and it has been shown that LBM introduces an advantage from the computational costs point of view - due to its intrinsic potential for parallel processing - see the following points

- **PBR simulation prototype**

  I have developed a simulation software prototype based on the proposed unified general framework for PBR modeling and successfully validated it on the case of the Couetter-Taylor photobioreactor (CTBR).

  Implemented software simulates the microalgal growth through the coupled LBM and PSF simulation and has been successfully validated as demonstrated in paper III, where the PSF model results and LBM results have been validated against analytic solutions of the simpler flow regimes/steady irradiance conditions.

- **Performance optimization - parallel processing**

  In order to prove the performance advantage of the proposed approach, I have also reimplemented the simulation software prototype on the parallel architecture of CUDA and successfully validated against the unparallelized implementation and analytic solutions of the simpler scenarios. The current parallel implementation of the solver shows approximately 20 times better performance when compared to the single threaded CPU implementation, thus introducing an important advantage by decreasing significantly the iteration cycle time in the PBR design process.

- **Evaluation of the transport modeling alternatives**

  Apart from the LBM based PBR transport model I have also developed a novel stochastic PBR modeling approach based on the random walk (RW). I have also implemented a working software prototype and successfully validated it against a Finite Difference Method (FDM) based model. It has been shown that the RW based model coupled to the real hydrodynamics by the means of the turbulent diffusion/spatially dependent dispersion coefficient is a viable alternative to the solution of the transport, or more correctly to the trajectories determination of the dispersed solid phase.

Future goals

Although a major progress in the field of PBR simulating software developement was made and presented in this thesis, further research based on the results from this work is required in order to obtain a general PBR design software, namely in the following areas:

- **Generalization of the software prototype** - the simulation software should be further generalized in order to be capable to simulate a custom geometry PBR
- **Further performance optimization/supercomputing architectures** - the current potential of the modern supercomputers should allow for another significant iteration cycle reduction in the PBR design process. It has been shown that the proposed framework copes well with the parallel architectures and this would be the next logical step.
- **Experimental verification** - in order to give more credibility to the general PBR simulation software, certainly more laboratory experiments regarding microalgal growth under various operating conditions should be performed and demonstrated in relation to the simulated results.

Appendix A

Selected source codes

In the scope of the thesis a coupled LBM/PSF photobioreactor simulation prototype has been implemented on the parallel architecture of CUDA. In this appendix, some of the related source codes and their outlines are presented.

A.1 LBM simulation

Simulation step consists of the invocation of the several CUDA kernels (see further) as outlined by the following source code (abbreviated):

```
void lbmSimulationStep(void) {

        preStreaming();
        kern_boundaries<<<grid, block>>>(...);
        CUSAFE(cudaThreadSynchronize());
        postStreaming();

        preStreaming();
        kern_streaming<<<grid, block>>>(...);
        CUSAFE(cudaThreadSynchronize());
        postStreaming();

        kern_updateMacroVariables<<<grid, block>>>(...);
        CUSAFE(cudaThreadSynchronize());

        kern_collissions<<<grid, block>>>();
        CUSAFE(cudaThreadSynchronize());
}
```

A.1.1 Streaming kernel

The streaming kernel of the LBM simulation leverages the 3D textures for better performance due to the spatially local caching - memory blocks for individual micro flow densities are mapped as 3D textures before being streamed to the adjacent node locations by the following CUDA kernel:

```
__global__ void kern_streaming(...) {

  int sliceHeightInBlocks = domainHeight/blockDim.y;
  int x = blockIdx.x * blockDim.x + threadIdx.x;
  int y = ((blockIdx.y%(sliceHeightInBlocks)) * blockDim.y +
      threadIdx.y);
  int z = blockIdx.y/(sliceHeightInBlocks)*blockDim.z+threadIdx.z;

  int idx = (z*domainHeight+y)*floatsPerLine + x;

  d_f1[idx] = tex3D(d_f1_txt, (float) (x-1), (float) y, (float)z);
  d_f2[idx] = tex3D(d_f2_txt, (float) (x+1), (float) y, (float)z);

  d_f3[idx] = tex3D(d_f3_txt, (float) x, (float) y, (float)(z-1));
  d_f4[idx] = tex3D(d_f4_txt, (float) x, (float) y, (float)(z+1));

  d_f5[idx] = tex3D(d_f5_txt, (float) x, (float) (y-1), (float)z);
  d_f6[idx] = tex3D(d_f6_txt, (float) x, (float) (y+1), (float)z);

  d_f7[idx] = tex3D(d_f7_txt, (float) (x-1), (float) y, (float)(z
      -1));
  d_f8[idx] = tex3D(d_f8_txt, (float) (x-1), (float) y, (float)(z
      +1));

  d_f9[idx] = tex3D(d_f9_txt, (float) (x-1), (float) (y-1), (float)
      z);
  d_f10[idx] = tex3D(d_f10_txt, (float) (x-1), (float) (y+1), (
      float)z);

  d_f11[idx] = tex3D(d_f11_txt, (float) (x+1), (float) y, (float)(z
      -1));
  d_f12[idx] = tex3D(d_f12_txt, (float) (x+1), (float) y, (float)(z
      +1));

  d_f13[idx] = tex3D(d_f13_txt, (float) (x+1), (float) (y-1), (
      float)z);
  d_f14[idx] = tex3D(d_f14_txt, (float) (x+1), (float) (y+1), (
      float)z);

  d_f15[idx] = tex3D(d_f15_txt, (float) x, (float) (y-1), (float)(z
      -1));
```

```
  d_f16[idx] = tex3D(d_f16_txt, (float) x, (float) (y+1), (float)(z
      -1));

  d_f17[idx] = tex3D(d_f17_txt, (float) x, (float) (y-1), (float)(z
      +1));
  d_f18[idx] = tex3D(d_f18_txt, (float) x, (float) (y+1), (float)(z
      +1));
}
```

A.1.2 Collision kernel

```
__global__ void kern_collissions(...) {

  int sliceHeightInBlocks = domainHeight/blockDim.y;
  int x = blockIdx.x * blockDim.x + threadIdx.x;
  int y = ((blockIdx.y%(sliceHeightInBlocks)) * blockDim.y +
      threadIdx.y);
  int z = blockIdx.y/(sliceHeightInBlocks)*blockDim.z+threadIdx.z;

  int nodeType = d_nodeTypes[(z*domainHeight+y)*intsPerLine+ x];

  if (nodeType != NT_COMMON && nodeType 1= NT_PERIODIC) {
      return;
  }

  int idx = (z*domainHeight+y)*floatsPerLine + x;

  float rho = d_macroDensities[idx];
  float vx = d_velocityComponentsX[idx];
  float vy = d_velocityComponentsY[idx];
  float vz = d_velocityComponentsZ[idx];

  float Bvxsq = vx * vx;
  float Bvysq = vy * vy;
  float Bvzsq = vz * vz;
  float BxyAsq = 4.5*(vx+vy)*(vx+vy);
  float BxyDsq = 4.5*(vx-vy)*(vx-vy);
  float BxzAsq = 4.5*(vx+vz)*(vx+vz);
  float BxzDsq = 4.5*(vx-vz)*(vx-vz);
  float ByzAsq = 4.5*(vy+vz)*(vy+vz);
  float ByzDsq = 4.5*(vy-vz)*(vy-vz);

  float C = 1.5*(vx*vx+vy*vy+vz*vz);

  d_f1[idx]=(1-invTau)*d_f1[idx] + invTau * (rho*EQ_COEF_1_6* (1+3*
      vx+Bvxsq-C));
```

```
  d_f2[idx]=(1-invTau)*d_f2[idx] + invTau * (rho*EQ_COEF_1_6* (1-3*
      vx+Bvxsq-C));

  d_f3[idx]=(1-invTau)*d_f3[idx] + invTau * (rho*EQ_COEF_1_6* (1+3*
      vz+Bvzsq-C));
  d_f4[idx]=(1-invTau)*d_f4[idx] + invTau * (rho*EQ_COEF_1_6* (1-3*
      vz+Bvzsq-C));

  d_f5[idx]=(1-invTau)*d_f5[idx] + invTau * (rho*EQ_COEF_1_6* (1+3*
      vy+Bvysq-C));
  d_f6[idx]=(1-invTau)*d_f6[idx] + invTau * (rho*EQ_COEF_1_6* (1-3*
      vy+Bvysq-C));

  d_f7[idx]=(1-invTau)*d_f7[idx] + invTau * (rho*EQ_COEF_7_18*
      (1+3*(vx+vz)+BxzAsq-C));
  d_f8[idx]=(1-invTau)*d_f8[idx] + invTau * (rho*EQ_COEF_7_18*
      (1+3*(vx-vz)+BxzDsq-C));

  d_f9[idx]=(1-invTau)*d_f9[idx] + invTau * (rho*EQ_COEF_7_18*
      (1+3*(vx+vy)+BxyAsq-C));
  d_f10[idx]=(1-invTau)*d_f10[idx] + invTau * (rho*EQ_COEF_7_18*
      (1+3*(vx-vy)+BxyDsq-C));

  d_f11[idx]=(1-invTau)*d_f11[idx] + invTau * (rho*EQ_COEF_7_18*
      (1-3*(vx-vz)+BxzDsq-C));
  d_f12[idx]=(1-invTau)*d_f12[idx] + invTau * (rho*EQ_COEF_7_18*
      (1-3*(vx+vz)+BxzAsq-C));

  d_f13[idx]=(1-invTau)*d_f13[idx] + invTau * (rho*EQ_COEF_7_18*
      (1-3 *(vx-vy)+BxyDsq-C));
  d_f14[idx]=(1-invTau)*d_f14[idx] + invTau * (rho*EQ_COEF_7_18*
      (1-3 *(vx+vy)+BxyAsq-C));

  d_f15[idx]=(1-invTau)*d_f15[idx] + invTau * (rho*EQ_COEF_7_18*
      (1+3 *(vz+vy)+ByzAsq-C));
  d_f16[idx]=(1-invTau)*d_f16[idx] + invTau * (rho*EQ_COEF_7_18*
      (1+3 *(vz-vy)+ByzDsq-C));

  d_f17[idx]=(1-invTau)*d_f17[idx] + invTau * (rho*EQ_COEF_7_18*
      (1-3 *(vz-vy)+ByzDsq-C));
  d_f18[idx]=(1-invTau)*d_f18[idx] + invTau * (rho*EQ_COEF_7_18*
      (1-3 *(vz+vy)+ByzAsq-C));

  d_f19[idx]=(1-invTau)*d_f19[idx] + invTau * (rho*EQ_COEF_19* (1-C
      ));
}
```

A.1.3 Boundaries kernel

Apart from the basic boundary conditions like bounce back, periodic etc... an interpolation boundary scheme based on [83] has been implemented and validated in paper [36]:

```
__device__ void interpolate(...) {

  float xb = x - (domainWidth-1)/2.0;
  float zb = z - (domainDepth-1)/2.0;

  int targetNodeType  = tex3D(d_nodeTypes_txt, (float) (x+elx), (
      float) y+ely, (float)z+elz);

  if (targetNodeType != NT_COMMON) {
   return;
  }

  float B = 2*xb*elx+2*zb*elz;
  float A = elx*elx+elz*elz;
  float C = xb*xb+zb*zb-innerRadiusInNodes*innerRadiusInNodes;

  float D = B*B-4*A*C;

  float k1 = (-B+sqrtf(D))/(2*A);
  float k2 = (-B-sqrtf(D))/(2*A);

  //we want to go in the direction of the unit vector -> let's
      select the positive k
  float k = (k1<0||(k2>0&&k1>k2))?k2:k1;
  float SIGMA = 1-k;

  float xw = xb + elx*k;
  float zw = zb + elz*k;

  float phi = 0;
  if (xw==0&&zw==0) {
    phi = 0;
  } else if (xw<=0) {
    phi = asinf(zw/innerRadiusInNodes);
  } else {
    phi = -asinf(zw/innerRadiusInNodes)+CUDART_PI_F;
  }

  float Uwx = omega * innerRadiusInNodes *sinf(phi);
  float Uwy = 0.0;
  float Uwz = omega * innerRadiusInNodes *cosf(phi);
```

```
float Ufx = tex3D(d_velocityComponentsX_txt, x+elx, y+ely, z+elz)
    ;
float Ufy = tex3D(d_velocityComponentsY_txt, x+elx, y+ely, z+elz)
    ;
float Ufz = tex3D(d_velocityComponentsZ_txt, x+elx, y+ely, z+elz)
    ;

float chi, Ubfx, Ubfy, Ubfz;

if (SIGMA<0.5) {
  chi = (2*SIGMA-1)/(tau-2);
  Ubfx = tex3D(d_velocityComponentsX_txt, x+2*elx, y+2*ely, z+2*
      elz);
  Ubfy = tex3D(d_velocityComponentsY_txt, x+2*elx, y+2*ely, z+2*
      elz);
  Ubfz = tex3D(d_velocityComponentsZ_txt, x+2*elx, y+2*ely, z+2*
      elz);
} else {
  chi = (2*SIGMA-1)/(tau+0.5);
  Ubfx = (1-3/(2*SIGMA))*Ufx+3/(2*SIGMA)*Uwx;
  Ubfy = (1-3/(2*SIGMA))*Ufy+3/(2*SIGMA)*Uwy;
  Ubfz = (1-3/(2*SIGMA))*Ufz+3/(2*SIGMA)*Uwz;
}


int outIdx = (z*domainHeight+y)*floatsPerLine+x;
float density = tex3D(d_macroDensities_txt, x+elx, y+ely, z+elz);
float f1f = tex3D(d_f1_txt, x+elx, y+ely, z+elz);
float f2f = tex3D(d_f2_txt, x+elx, y+ely, z+elz);
float f3f = tex3D(d_f3_txt, x+elx, y+ely, z+elz);
float f4f = tex3D(d_f4_txt, x+elx, y+ely, z+elz);
float f5f = tex3D(d_f5_txt, x+elx, y+ely, z+elz);
float f6f = tex3D(d_f6_txt, x+elx, y+ely, z+elz);
float f7f = tex3D(d_f7_txt, x+elx, y+ely, z+elz);
float f8f = tex3D(d_f8_txt, x+elx, y+ely, z+elz);
float f9f = tex3D(d_f9_txt, x+elx, y+ely, z+elz);
float f10f = tex3D(d_f10_txt, x+elx, y+ely, z+elz);
float f11f = tex3D(d_f11_txt, x+elx, y+ely, z+elz);
float f12f = tex3D(d_f12_txt, x+elx, y+ely, z+elz);
float f13f = tex3D(d_f13_txt, x+elx, y+ely, z+elz);
float f14f = tex3D(d_f14_txt, x+elx, y+ely, z+elz);
float f15f = tex3D(d_f15_txt, x+elx, y+ely, z+elz);
float f16f = tex3D(d_f16_txt, x+elx, y+ely, z+elz);
float f17f = tex3D(d_f17_txt, x+elx, y+ely, z+elz);
float f18f = tex3D(d_f18_txt, x+elx, y+ely, z+elz);

float vXf = (f1f +f7f+f8f+f9f+f10f  -(f2f+f11f+f12f+f13f+f14f))/
    density;
```

```
  float vYf = (f5f +f13f+f15f+f17f+f9f  -(f6f+f10f+f14f+f16f+f18f))
      /density;
  float vZf = (f3f +f7f+f11f+f15f+f16f  -(f4f+f8f+f12f+f17f+f18f))/
      density;

  float d_fInEq = computeEQ(weight, -elx, -ely, -elz, Ufx, Ufy, Ufz
      , density);

  float fin = tex3D(d_fIn_txt, x+elx, y+ely, z+elz);

  d_fOut[outIdx] = fin-chi*(fin-d_fInEq)+density*weight*3*
    (
      -elx*(chi*(Ubfx-Ufx)-2*Uwx)
      -ely*(chi*(Ubfy-Ufy)-2*Uwy)
      -elz*(chi*(Ubfz-Ufz)-2*Uwz)
    );
}

__device__ __inline__ float computeEQ(
                float weight,
                int elx, int ely, int elz,
                float velX, float velY, float velZ,
                float density) {
        return weight*density*
                (
                        1
                        +3*(elx*velX+ely*velY+elz*velZ)
                        +4.5*(elx*velX+ely*velY+elz*velZ)*(elx*velX
                            +ely*velY+elz*velZ)
                        -1.5*(velX+velY+velZ)*(velX+velY+velZ));
}
```

A.2 PSF Simulation

PSF simulation is based on a Lagrangian model where the dispersed solid phase is tracked as individual particles as described and validated against analytic solutions of the PSF model in [36]:

```
__global__ void kern_updatePhotoStates(...) {

  int particleId = threadIdx.x + blockDim.x *blockIdx.x;

  curandState randState = d_curandStates[particleId];
  float uniRand = curand_uniform(&randState);

  int currentState = d_particlePhotoStates[particleId];
```

```
  int newState = currentState;

  float particlePositionY_LU = d_particlePositionsY[particleId];
  float particleDistanceFromSource_m = particlePositionY_LU *
      physicalHeight/(float)heightInNodes;
  float lightIntensity = surfaceLightIntensity * exp(-attenuation*
      particleDistanceFromSource_m);

  float r2AThreshold=alpha*lightIntensity*timeStep;
  float a2IThreshold=(gamma+beta*lightIntensity)*timeStep;

  if (currentState == ACTIVATED) {
    if (uniRand<=a2RThreshold) {
      newState=RESTING;
    } else if (uniRand <= a2IThreshold) {
      newState=INHIBITED;
    }
  } else if (currentState == INHIBITED) {
    if (uniRand<=i2RThreshold) {
      newState=RESTING;
    }
  } else if (uniRand<=r2AThreshold) {
    newState=ACTIVATED;
  }


  d_curandStates[particleId] = randState;
  d_particleActivatedCounter[particleId] += ((newState == ACTIVATED
      )?1:0);
  d_particlePhotoStates[particleId] = newState;
}
```

Appendix B

List of abbreviations

Abbreviations

Abbreviation	Meaning
BC	Boundary condition
BGK	BhatnagarGrossKrook LBM collision model
CAD	Computer Aided Design
CFD	Computational fluid dynamics
CPU	Central Processing Unit
CTBR	Couette-Taylor Photobioreactor
CUDA	Compute Unified Device Architecture
D3Q19	three-dimensional 19 velocity LBM lattice
DNS	Direct Numerical Simulation
DRW	Discrete Random Walk
FDM	Finite difference method
FEM	Finite element method
FVM	Finite volume method
GPU	Graphics Processing Unit
LBM	Lattice-Boltzmann Method for fluid flow
LES	Large Eddy Simulation
ODE, PDE (s)	Ordinary/partial differential equation(s)
PBR	Photobioreactor
PRNG	Parallel Random Number Generator
PSF	Photosynthetic factory
RANS	Reynolds-Averaged Navier-Stokes
RNG	Random Number Generator
RW	Random Walk
SRT	Single Relaxation Time LBM model

References

[1] Metting, F.B. (1996). Biodiversity and application of microalgae. *Journal of Industrial Microbiology and Biotechnology*, 17 (5–6), 477–489.

[2] Singh S., Kate B.N., Banerjee, U.C. (2005). Bioactive compounds from cyanobacteria and microalgae: an overview. *Critical Reviews in Biotechnology*, 25 (3), 73–95.

[3] Plaza M., Santoyo S., Jaime L., García-Blairsy Reina G., Herrero M., Señoráns F.J., Ibáñez E. (2010). Screening for bioactive compounds from algae *Journal of Pharmaceutical and Biomedical Analysis*, 51, 450–455

[4] Chisti Y. (2007). Biodiesel from microalgae. *Biotechnology Advances*, 25, 294–306.

[5] Brennan L., Owende P. (2010). Biofuels from microalgaeA review of technologies for production, processing, and extractions of biofuels and coproducts. *Renewable and Sustainable Energy Reviews*, 14 (2), 557–577.

[6] Rath B. (2011). Microalgal bioremediation : Current practices and perspectives. *Journal of Biochemical Technology*, 3 (3), 299–304.

[7] Borowitzka M. A. (1997). Microalgae for aquaculture: Opportunities and constraints. *Journal of Applied Phycology*, 9 (5), 393–401.

[8] Spolaore P., Joannis-Cassan, C., Duran E., Isambert A. (2006). Commercial applications of microalgae. *Journal of Bioscience and Bioengineering* 101 (2), 87–96.

[9] Borowitzka M.A. (1999). Commercial production of microalgae: ponds, tanks, tubes and fermenters. *Journal of Biotechnology*, 70, 313–321

[10] Richmond, A. (2004). Biological Principles of Mass Cultivation. In: *Handbook of Microalgal Culture: Biotechnology and Applied Phycology*, A. Richmond, Ed., Blackwell Publishing, 125–177.

[11] Schugerl K., Bellgardt K.-H. (Eds) (2000) *Bioreaction Engineering, Modeling and Control.* Springer-Verlag, Berlin, Heidelberg.

[12] Cornet, J.-F., Dussap C.G., Gros J.-B. (1994). Conversion of radiant light energy in photobioreactors. *A.I.Ch.E. journal*, 40, 1055–1066.

[13] Cornet, J.-F., Dussap C.G., Gros J.-B., Binois C., Lasseur C. (1995). A simplified monodimensional approach for modeling coupling between radiant light transfer and growth kinetics in photobioreactors. *Chemical engineering science*, 50, 1489–1500.

[14] Cornet J.-F., Albiol J. (2000) Modeling photoheterotrophic growth kinetics of *Rhodospirullum rubrum* in rectangular photobioreactors. *Biotechnology Progress*, 16, 199–207.

[15] Berberoglu H., Yin J., Pilon L. (2007) Light transfer in bubble sparged photobioreactors for H2 production and CO2 mitigation. *Int J Hydrogen Energy*, 32, 2273–2285.

[16] Bosma R., van Zessen E., Reith J.H., Tramper J., Wijffels R.H. (2007) Prediction of volumetric productivity of an outdoor photobioreactor. *Biotechnol Bioeng*, 97, 1108–1120

[17] Nedbal L., Tichý V., Xiong F., Grobbekaar J.U. (1996) Microscopic green algae and cyanobacteria in high-frequency intermittent light. *J Appl Phycol*, 8, 325–333

[18] Camacho Rubio F., Camacho F.G., Sevilla J.M.F., Chisti Y., Molina Grima E. (2003) A mechanistic model of photosynthesis in microalgae. *Biotechnol Bioeng*, 81, 473–559

[19] Kroon B.M.A. (1994) Variability of photosystem II quantum yield and related processes in *Chlorella pyrenoidosa* (Chlorophyta) acclimated to an oscillating light regime simulating a mixed photic zone. *J. Phycol.*, 30, 841–852.

[20] Terry K.L. (1986) Photosynthesis in modulated light: Quantitative dependence of photosynthetic enhancement on flashing rate. *Biotechnol Bioeng* 28, 988–995.

[21] Molina E., Fernandez J., Acien F.G., Chisti Y. (1999) Photobioreactors: light regime, mass transfer and scaleup. *Journal of Applied Phycology*, 12, 355–368

[22] Eriksen N. T. (2008) The technology of microalgal culturing. *Biotechnol Lett*, 30, 1525–1536

[23] Miller R., Tsuchiya H., Fredrickson A., Brown A. (1964) Hydromechanical method to increase efficiency of algal photosynthesis. *Ind Eng Chem Proc Des Dev*, 3, 134–143

[24] Contreras Gomez A., Garcia Camacho F., Molina Grima E., Merchuk J.C. (1998) Interaction between CO2-mass transfer, light availability, and hydrodynamic stress in the growth of Phaeodactylum tricornutum in a concentric tube airlift photobioreactor. *Biotechnol Bioeng ng*, 60, 317-325.

[25] Michiel H.A. Michels, Atze J. van der Goot, Norsker N.-H., wijffels R.H. (2010) Effects of shear stress on the microalgae *Chaetoceros muelleri*. *Bioprocess Biosyst. Eng.*, 33, 921–927

[26] Barbosa M.J., Albrecht M., Wijffels R.H. (2003) Hydrodynamic stress and lethal events in sparged microalgae cultures. *Biotechnol Bioeng*, 83, 112–120

[27] Vega-Estrada J., Montes-Horcasitas M.C., Domínguez-Bocanegra A.R., Cañizares-Villanueva R.O. (2005) Haematococcus pluvialis cultivation in split-cylinder internal-loop airlift photobioreactor under aeration conditions avoiding cell damage. *Appl Microbiol Biotechnol*, 68, 31–35

[28] Ben-Amotz A., Avron M. (1992) *Dunaliella: physiology, biochemistry, and biotechnology* CRC press.

[29] Masojídek J., Kopecký J., Giannnelli L., Torzillo G. (2011) Productivity correlated to photobiochemical performance of Chlorella mass cultures grown outdoors in thin-layer cascades. *J Ind Microbiol Biotechnol.*, 38 (2), 307–317

[30] Mirón A.S., Camacho F.G., Gómez A.C., Grima E.M., Chisti Y. (2000) Bubble-column and airlift photobioreactors for algal culture. *AIChe Journal*, 46, 1872–1887

[31] Schenk P. M., Thomas-Hall S. R., Stephens, E., Marx, U. C., Mussgnug, J. H., Posten, C., Kruse, O., Hankamer, B. (2008). Second generation biofuels:

High-efficiency microalgae for biodiesel production. *Bioenergy Res.*, 1 (1), 1939–1234.

[32] Carvalho A.P., Meireles L.A., Malcata F.X. (2006) Microalgal reactors: a review of enclosed system designs and performances. *Biotechnol Prog*, 22(6), 1490-1506.

[33] Papáček Š., Matonoha C., Štumbauer V., Štys D. (2012) Modelling and simulation of photosynthetic microorganism growth: random walk vs. finite difference method. *Mathematics and Computers in Simulation*, 10 (82), 2022–2032

[34] Papáček Š. (2005) Photobioreactors for cultivation of microalgae under strong irradiances: Modelling, simulation and design. *Ph.D. Thesis, Faculty of Mechatronics and Interdisciplinary Engineering Studies, Technical University of Liberec*

[35] Papáček Š., Štumbauer V., Štys D., Petera K., Matonoha C. (2011) Growth impact of hydrodynamic dispersion in a Couette-Taylor bioreactor. *Mathematical and Computer Modelling*, 7-8 (54), 1791–1795.

[36] Štumbauer V., Petera K., Štys D. (2013) Lattice Boltzmann method in bioreactor design and simulation. *Mathematical and Computer Modelling*, 7-8 (57), 1913-1918

[37] Taylor G. I. (1923) Stability of a viscous liquid contained between two rotating cylinders. *Philos. Trans. R. Soc. London Ser A.*, 223, 289

[38] Wang L., Olsen M., Vigil R. (2005) Reappearance of azimuthal waves in turbulent Taylor-Couette flow at large aspect ratio. *Chem Eng Sci*, 60, 5555–5568

[39] Antonijoan J., Sánchez J. (2002) On stable Taylor vortices above the transition to wavy vortices. *Physics of Fluids*, 14, 1661

[40] Renaud S. M., Luong-Van Thinh, Lambrinidis G., Parry D. L. (2002) Effect of temperature on growth, chemical composition and fatty acid composition of tropical Australian microalgae grown in batch cultures. *Aquaculture*, 211, 195–214

[41] Lamers P.P., Carlien C.W. van de Laak, Kaasenbrood P.S., Lorier J., Janssen M., Ric De Vos C.H., Bino R.J., Wijffels R.H. (2010) Carotenoid

and fatty acid metabolism in light-stressed Dunaliella salina. *Biotechnology and Bioengineering*, 4 (106), 638–648.

[42] Dunn I.J., Heinzle E., Ingham J., Přenosil J.E. (1992) *Biological reaction engineering* VCH, Weinheim-New York-Basel-Cambridge

[43] Eilers P.H.C., Peeters J.C.H. (1988) A model for the relationship between light intensity and the rate of photosynthesis in phytoplankton. *Ecological Modelling*, 42, 199–215.

[44] Eilers P.H.C., Peeters J.C.H. (1993) Dynamic behaviour of a model for photosynthesis and photoinhibition. *Ecological Modelling*, 69 , 113–133.

[45] Wu X., Merchuk J.C. (2001) A model integrating fluid dynamics in photosynthesis and photoinhibition processes. *Chemical Engineering Science*, 56, 3527–3538.

[46] Papáček Š., Štys D., Dolínek P., Petera K. (2007) Multicompartment/CFD modelling of transport and reaction processes in Couette-Taylor photobioreactor. *Applied and Computational Mechanics*, 1, 577–586

[47] Succi S. (2001) The Lattice Boltzmann Equation for Fluid Dynamics and Beyond. Oxford University Press

[48] Sukop M. C., Thorne D. T. (2007) Lattice Boltzmann modeling: an introduction for geoscientists and engineers. Springer.

[49] Qian Y.H., d'Humieres D., Lallemand P. (1992) Lattice BGK models for Navier-Stokes equation. *Europhys Lett*, 17, 479–484

[50] Gallivan M.A., Noble D.R., Georgiadis J.G., Buckius R.O. (1997) An evaluation of the bounce-back boundary condition for lattice Boltzmann simulations. *Int J Num Meth Fluids*, 25, 249–263.

[51] Inamuro T., Yoshino M., Ogino F. (1995) A non-slip boundary condition for the lattice Boltzmann simulations. *Phys Fluids*, 7, 2928–2930.

[52] Chen S., Martínez D, Mei R. (1996) On boundary conditions in lattice Boltzmann methods. *Phys Fluids*, 8, 2527–2536.

[53] Zou Q., He X. (1997) On the pressure and velocity boundary conditions for the lattice Boltzmann BGK model. *Phys Fluids*, 9, 1591–1598.

[54] Shan X. Chen H. (1994) Simulation of nonideal gases and liquid-gas phase transitions by the lattice Boltzmann equation. *Phys Rev E*, 49, 2941–2948.

[55] Hyväluoma J., Raiskinmäki P., Jäsberg A., Koponen A., Kajata M., Timonen J. (2004) Evaluation of a lattice-Boltzmann method for mercury intrusion porosimetry simulations. *Future Generation Computer Systems*, 20, 1003-1011.

[56] Qian Y.H., Succi S., Orszag S.A. (1995) Recent advances in lattice Boltzmann computing. *Ann Rev Comp Phys*, 30, 195-242.

[57] Mohamad A.A. (2011) Lattice Boltzmann Method *Fundamentals and Engineering Applications with Computer Codes* Springer-Verlag London Limited, ISBN 978-0-85729-454-8.

[58] Dolínek P. (2007) Couette-Taylor Photobioreactor. Master thesis, faculty of mechanical engineering, Czech Technical University.

[59] Wu X., Merhuck J.C. (2002) Simulation of algae growth in a bench-scale bubble column reactor. *Biotechnol. Bioeng.*, 80 (2), 156–68.

[60] Eteshola E., Karpasas M., Arad (Malis) S., Gottlieb M. (1998) Red microalga polysaccharades. 2. Study of the rheology, morphology and thermal relations of aqueous preparations. *Acta Polym*, 49, 549–556.

[61] Merchuk, J.C., Gluz M., Mukmenev I. (2000) Comparison of photobioreactors for the cultivation of the microalga *Porphyridium sp.*. *J. Chem. technol. Biotechnol.*, 57 (12), 1119–1126.

[62] ANSYS, Inc. (2011) ANSYS FLUENT Theory Guide. Release 14.0 (November 2011).

[63] Michele V., Hempel D.C. (2002) Liquid flow and phase holdup-measurement and CFD modeling for two-and three-phase bubble columns. *Chemical Engineering Science*, 57, 1899–1908.

[64] Qiang, H., Richmond, A. (1996). Productivity and photosynthetic efficiency of Spirulina platensis as affected by light intensity, algal density and rate of mixing in a flat plate photobioreactor. *Journal of Applied Phycology*, 8, 139–145.

[65] Nedbal L., Tichý V., Xiong F., Grobbelaar J.U. (1996) Microscopic green algae and cyanobacteria in high-frequency intermittent light. *J. Appl. Phycol.*, 8, 325–333.

[66] Papáček Š., Čelikovský S., Štys D., Ruiz-León J. (2007) Bilinear System as Modelling Framework for Analysis of Microalgal Growth. *Kybernetika*, vol. 43, 1–20.

[67] Papáček Š., Čelikovský S., Rehák B., Štys D. (2010) Experimental design for parameter estimation of two time-scale model of photosynthesis and photoinhibition in microalgae. *Mathematics and Computers in Simulation*, 80, 1302–1309

[68] Rehák, B., Čelikovský S., Papáček, Š. (2008) Model for Photosynthesis and Photoinhibition: Parameter Identification Based on the Harmonic Irradiation O_2 Response Measurement. Joint Special Issue of *TAC IEEE* and *TCAS IEEE*, 101–108

[69] Čelikovský S., Papáček, Š., Cervantes-Herrera A., Ruiz-León J. (2010) Singular perturbation based solution to optimal microalgal growth and its infinite time horizon analysis. *TAC IEEE*, 55 (3), 767–772

[70] Molina E., Acien F.G., Garcia F., Camacho F., Chisti Y. (2000) Scale-up of tubular photobioreactors. *Journal of Biotechnology*, 92, 113–131

[71] Mann R., Mavros P. (1982) Analysis of unsteady tracer dispersion and mixing in a stirred tank vessel using interconnected networks of ideal flow zones. *Papers presented at the 4th European conference on mixing*, Noordwijkerhout, The Netherlands, 35–47.

[72] Mann R., Knysh P., Rasekoala E.A., Didari M. (1987) Mixing in a closed stirred vessel: Use of network zones to interpret mixing in a closed stirred vessel. *Fluid mixing: Vol III. International Chemical Engineering Symposium Series*, 108, 49–60.

[73] Vlaev D., Mann R., Lossev V.,Vlaev S.V., Zahradnik J.,Seichter P. (2000) Macro-mixing and *Streptomyces Fradiae*. Modelling oxygen and nutrient segregation in an industrial bioreactor. *Chemical Engineering, Research and Design*, 78, 354–362.

[74] Bezzo F., Macchietto S., Pantelides C.C., (2003) General hybrid multizonal/CFD approach for bioreactor modeling *AICHE Journal*, 49, 2133–2148.

[75] Bezzo F., Macchietto S., Pantelides C.C. (2004) A general methodology for hybrid multizonal/CFD models - Part I. Theoretical framework *Computers & Chemical Engineering* 28, 501–511.

[76] Bezzo F., Macchietto S. (2004) A general methodology for hybrid multizonal/CFD models - Part II. Automatic zoning *Computers & Chemical Engineering*, 28, 513–525.

[77] Bezzo F., Macchietto S., Pantelides C.C. (2005) Computational issues in hybrid multizonal/computational fluid dynamics models *AIChE Journal*, 51, 1169–1177.

[78] Zhao L., Zhang Ch. (2013):A Parallel Unstructured Finite-Volume Method for All-Speed Flows *Numerical Heat Transfer, Part B: Fundamentals: An International Journal of Computation and Methodology*, 4 (65), 336–358.

[79] He X., Luo L. (1997):Lattice Boltzmann for the incompressible Navier-Stokes equation *J. Stat. Phys*, 3/4 (88), 336–358.

[80] NVIDIA Corporation (2014) NVIDIA CUDA C Programming Guide

[81] Thibault J. C., Senocak I. (2009) CUDA implementation of a Navier-Stokes solver on multi-GPU desktop platforms for incompressible flows. *In Proceedings of the 47th AIAA Aerospace Sciences Meeting*, 758

[82] Tölke J., Krafczyk M. (2008) TeraFLOP computing on a desktop PC with GPUs for 3D CFD. *International Journal of Computational Fluid Dynamics*, 22(7), 443–456.

[83] Mei R., Shyy W., Luo L.S.: Lattice Boltzmann method for 3D flows with curved boundary. *Journal of Computational Physics*, 161 (2000), 680–699

stumbav@gmail.com

Modeling, parameter estimation, optimization and control of transport and reaction processes in bioreactors
Ph.D. Thesis Series, 2016, No. 12

Printed in the Czech Republic by Typodesign
Edition of 10 copies

University of South Bohemia in české Budějovice
Faculty of Science
Branišovsk 1760
CZ-37005 České Budějovice, Czech Republic

Phone: +420 387 776 201
www.prf.jcu.cz, e-mail: sekret-fpr@prf.jcu.cz